JOC The Journal of Organic Chemistry

pubs.acs.org/joc Article

Structural Modifications of Nile Red Carbon Monoxide Fluorescent Probe: Sensing Mechanism and Applications

Dominik Madea, Marek Martínek, Lucie Muchová, Jiří Váňa, Libor Vítek, and Petr Klán*

Cite This: https://dx.doi.org/10.1021/acs.joc.9b03217 Read Online

ACCESS | Metrics & More | Article Recommendations | Supporting Information

ABSTRACT: Carbon monoxide (CO) is a cell-signaling molecule (gasotransmitter) produced endogenously by oxidative catabolism of heme, and the understanding of its spatial and temporal sensing at the cellular level is still an open challenge. Synthesis, optical properties, and study of the sensing mechanism of Nile red Pd-based CO chemosensors, structurally modified by core and bridge substituents, in methanol and aqueous solutions are reported in this work. The sensing fluorescence "off−on" response of palladacycle-based sensors possessing low-background fluorescence arises from their reaction with CO to release the corresponding highly fluorescent Nile red derivatives in the final step. Our mechanistic study showed that electron-withdrawing and electron-donating core substituents affect the rate-determining step of the reaction. More importantly, the substituents were found to have a substantial effect on the Nile red sensor fluorescence quantum yields, hereby defining the sensing detection limit. The highest overall fluorescence and sensing rate enhancements were found for a 2-hydroxy palladacycle derivative, which was used in subsequent biological studies on mouse hepatoma cells as it easily crosses the cell membrane and qualitatively traces the localization of CO within the intracellular compartment with the linear quantitative response to increasing CO concentrations.

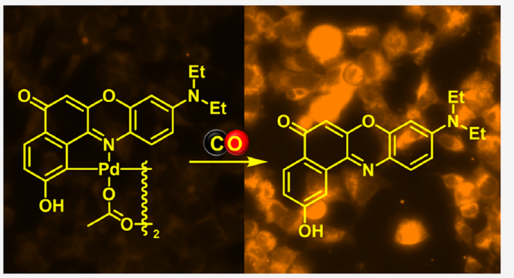

INTRODUCTION

Carbon monoxide (CO) is known for its toxic effects in mammals because its binding affinity for hemoglobin is over 200 times greater than that of molecular oxygen.[1,2] At low concentrations, CO acts as a cell-signaling molecule (gasotransmitter),[3] and it is produced endogenously by the oxidative catabolism of heme-by-heme oxygenase (HMOX-1) and, to some extent, by lipid peroxidation as well as gut microbiota.[4] It has been evidenced that CO is biologically relevant; it exhibits antiapoptotic, anti-inflammatory, antiproliferative, and anticoagulation effects[5−7] and prevention of tissue damage and cardiovascular pathology,[8] although the mechanisms are still not well understood. To utilize these potentially chemopreventive and/or therapeutic effects, CO-releasing molecules (CORMs) have been developed as artificial tools to deliver therapeutic amounts of CO into the cell using various initiation approaches.[7,9−16]

The increasing interest in CO as a signaling molecule has led to attempts to develop sensors, which detect, monitor, and quantify this gasotransmitter in biological samples, cells, and tissues. Many methods for the detection of exo- and endogenous CO in cells or living organisms have already been developed, especially in the past decade. Besides electrochemical,[17,18] infrared,[19] surface-enhanced Raman spectroscopy,[20] and colorimetric[21−23] methods, several fluorescent molecular chemosensors have been reported.[24,25] Chemosensors can provide a high spatio-temporal resolution of analytes.

CO sensing can be based on its interaction with transition-metal species, and two major detection mechanisms are recognized. The first process is a palladium-catalyzed substitution (Tsuji−Trost) reaction,[26−34] originally used for Pd^0 detection.[35,36] It is a catalytic, thus very sensitive process, but it requires introducing a second reaction component, a Pd^{II} salt (Scheme 1a). The second mechanism is the incorporation of CO into a palladacycle-based sensor that results in the liberation of Pd as a heavy atom responsible for initial fluorescence quenching of the sensor (Scheme 1b).[37−41] The latter systems are less sensitive but do not require the presence of any other reagent. The applications of palladacycle-based CO sensors are usually limited by their lower sensitivity, low aqueous solubility, and thermal instability. Only a few other reported CO chemosensors use different sensing mechanisms. Some of them are based on a steric hindrance associated with binding of CO to a transition metal.[42−44] Other examples of CO detection involve an azidocarbonylation reaction in the presence of a Pd catalyst[45,46] or utilize CO to reduce a nitro group into an amino group in the presence of a transition metal as catalyst.[47−51]

For this work, we selected one of the most promising fluorescent "off−on" probes based on a Nile red fluorophore

Received: November 28, 2019

Scheme 1. (a) Tsuji–Trost-Based Fluorescent CO Sensors; (b) Palladacycle-Based Fluorescent CO Sensors (a Simplification)

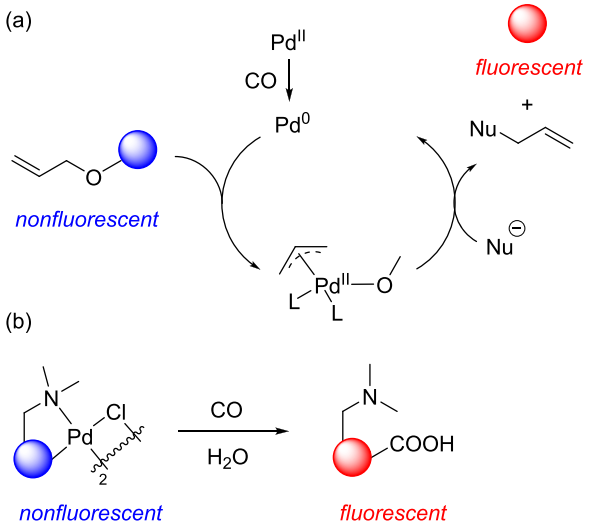

(9-diethylamino-5-benzo[*a*]phenoxazinone) reported by Lin and co-workers,[40] and we modified its structure to overcome some of its drawbacks, such as its lower sensitivity and poor solubility in water, to propose an improved CO sensor for human biology applications (Scheme 2). Our strategy involved

Scheme 2. Nile Red-Based CO Sensor (R_1, R_2 = H, X = CH_3COO)[40] and Its Modifications Reported in This Work

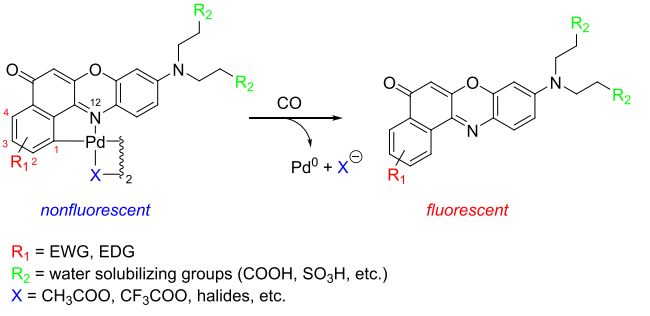

modifications of the bridged ligand X, different electron-withdrawing or electron-donating groups in the 2–4 positions of the Nile red core, and addition of water-solubilizing groups. Because a sensing mechanism of Nile red chemosensors has not been studied yet, we investigated the substituent effects on the mechanism of CO incorporation into a palladacycle and, subsequently, on the fluorescent probe release triggered by its reaction with CO using NMR, high resolution mass spectrometry (HRMS), and electrospray ionization mass spectrometry (ESI-MS) techniques. Finally, the biological usability of the selected sensor is demonstrated.

RESULTS AND DISCUSSION

Synthesis. 1,4-Epoxynaphthalene derivative **1** was treated with BF_3 to give synthetic intermediate 7-fluoronaphthalen-1-ol (**2**), formed as a major product in 44% yield along with its 6-fluoro isomer **3** (Scheme 3) according to Repine and co-workers.[52] Another building block, 8-fluoronaphthalen-1-ol **6**, was prepared via a three-step reaction reported by Cibulka[53] and Zhu,[54] involving compounds **4** and **5**, respectively, in the overall chemical yield of 29%. Aminophenols (**7**–**10**), synthesized as shown in Scheme 4, were used for the preparation of nitrosophenols **11a**–**c** using general procedure A, described in the Experimental Section (Scheme 5). The condensation of **11a**–**c** with the corresponding napthalene-1-ols in dimethylformamide (DMF) gave Nile red derivatives **12**–**14** (Scheme 6). Their isolated chemical yields were moderate to low (5–30%); they were lower especially in the case of more polar derivatives **13a,b** and **14a,b** after an indispensable repetitive purification process (column chromatography and recrystallization). The 3-methoxy derivative **15** was prepared by a subsequent methylation of **12d** in a good yield (69%).

Palladacycles **16**–**19** were synthesized from compounds **12**–**15** by C–H bond activation with $Pd(OAc)_2$ in acetic acid (Scheme 7) using modified procedures reported in the literature.[40,55,56] The amount of $Pd(OAc)_2$ (1–2 equiv) used was optimized. Residual Pd^{II} salt and/or unreacted starting material was removed by recrystallization to give palladacycles in 40–90% (**16a**–**c**, **19**) and 30–60% (**17a,b** and **18a,b**). The synthesis of 4-fluoro derivative **16e** was not successful; only a mixture of unidentified products was observed. The mechanism of C–H bond activation[57] resembles the electrophilic aromatic substitution; deactivation of a π-system by electron-withdrawing fluorine in the *para* position to the C–Pd bond may be detrimental for this reaction. 3-Fluoro derivative **16c** was successfully prepared in a lower yield (41%). Trifluoroacetate-bridged palladacycle **20** (Scheme 8) was prepared in a similar manner to palladacycles **16**–**19** in a good yield (60%) using trifluoroacetic acid as a solvent.

Palladacycles usually exist as dimers in both the solid state and solutions.[58] The NMR spectra of water-soluble derivatives (**17a,b**, **18a,b**) in D_2O were not resolved even at lower temperatures. The HRMS spectra of **16**–**20** (Figures S67–

Scheme 3. Synthesis of 7- and 8-Fluoronaphthalene-1-ols (2 and 6)

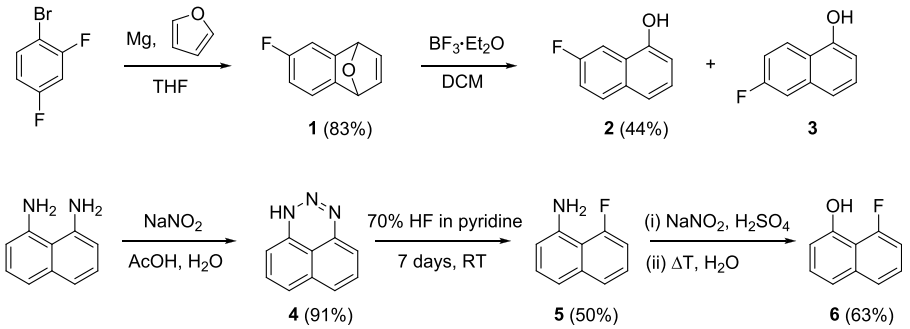

https://dx.doi.org/10.1021/acs.joc.9b03217
J. Org. Chem. XXXX, XXX, XXX–XXX

Scheme 4. Synthesis of Aminophenols 8 and 10

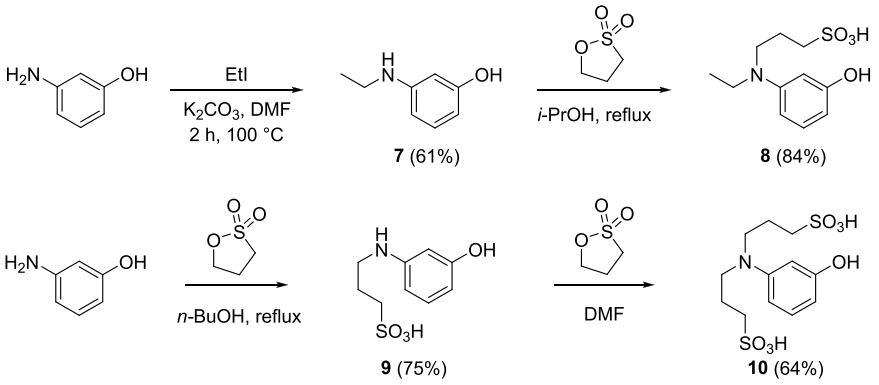

Scheme 5. Synthesis of Nitrosophenol Hydrochlorides 11a-c

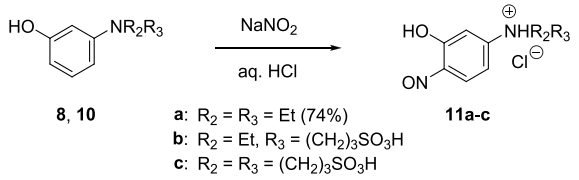

S74) showed signals of both the monomeric and dimeric forms in agreement with the literature,[41] although the dimer signals were negligible or even absent in some cases (Figures S68 and S72−S74). To gain further evidence that the prepared complexes exist as dimers, the bridge-splitting reaction of complexes **16a−c** and **20** with pyridine in dry dichloromethane as a noncoordinating solvent was studied.[59] Upon pyridine addition, the solutions of all palladacycles exhibited changes in their absorption spectra. The corresponding equilibrium constants were determined by titration and global fitting of the absorbance changes (Table 1 and Figures S80−S82). The equilibrium constant for the trifluoroacetate complex **20** could not be calculated because the bridge splitting with pyridine was quantitative.

Reaction of CO with Palladacycles 16−20. Initially, we identified products of the reaction of CO with palladacycles dissolved in methanol or phosphate-buffered saline (PBS). The less polar probes (**16a−c**, **19**, **20**) are not sufficiently soluble in water; thus, their reactions were studied in methanol. A solution of a palladacycle (**16a−c**) in methanol was stirred under a CO atmosphere for 16 h to give a methyl ester of carboxylic acid (**21a−c**) in quantitative yields (Scheme 9).

Scheme 7. Synthesis of Nile Red Palladacycles

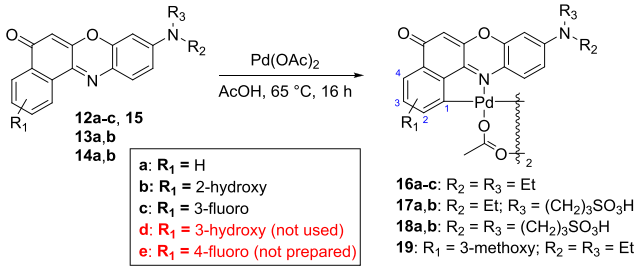

Scheme 8. Synthesis of Trifluoroacetate-Bridged Palladacycle 20

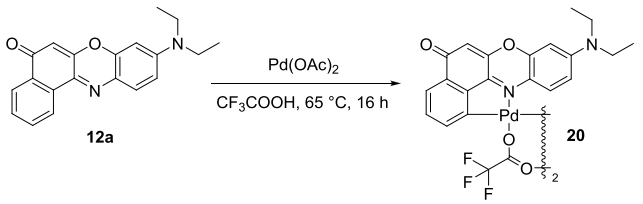

These products, along with Pd^0 black and acetic/trifluoroacetic acid byproducts, were formed via Pd-mediated carbonylation.[60−62] The reactions of palladacycles **19** and **20** resulted in a mixture of carbonylated (**22** and **21a**) and reduction (**15** and **12a**) side products, respectively, in the ratios of ∼1.5 : 1 (Figures S53 and S54). Therefore, compounds **19** and **20** were excluded from further studies.

More polar probes (**17a,b**, **18a,b**) are sufficiently soluble in PBS. A solution of a palladacycle (**17a**, ∼10 μM) in PBS was

Scheme 6. Synthesis of Nile Red Derivatives

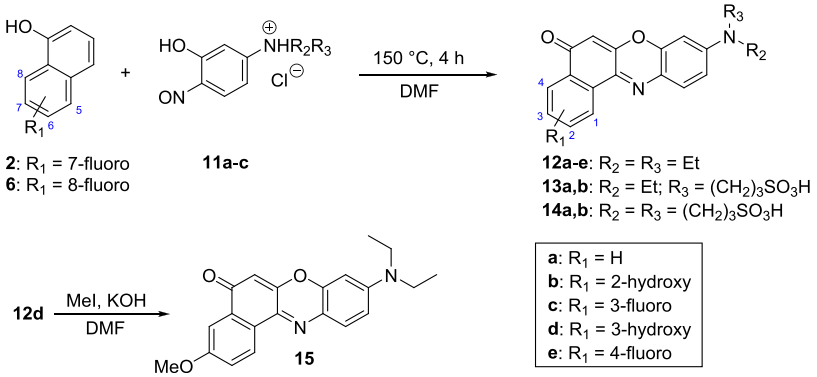

https://dx.doi.org/10.1021/acs.joc.9b03217
J. Org. Chem. XXXX, XXX, XXX−XXX

Table 1. Equilibrium Constants for the Bridge Splitting of 16a−c and 20 with Pyridine in Dry Dichloromethane

compd	$K^a = \frac{c_M^2}{c_D c_L^2}$
16a	3.8 ± 0.1[a]
16b	nd[b]
16c	6.6 ± 0.1
20	>10[3]

[a]Determined at 20.0 ± 0.1 °C. [b]A pyridine complex is not stable.

Scheme 9. Reaction of CO with Nile Red Palladacycles in Methanol and PBS

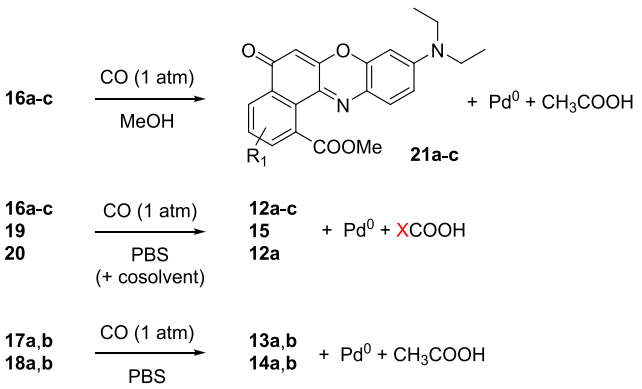

stirred under CO atmosphere for 16 h, and the reaction mixture was analyzed by high-performance liquid chromatography (HPLC) and HRMS. The reduction product, a Nile red derivative **13a**, was formed in >80% yield (HPLC, HRMS; Scheme 9 and Figure S58). This finding is in accordance with the observed reactivity of an unsubstituted derivative **16a**[56] and other palladacycles used as CO probes in aqueous solutions.[38−41] In contrast, a boron dipyrromethene (BODIPY)-derived Chang's probe (Figure 1)[37] gave a substituted

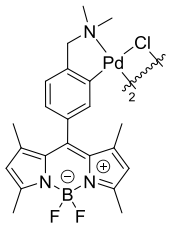

Figure 1. BODIPY-Based Probe for CO as Reported by Chang and Co-Workers.[37]

benzoic acid derivative instead. The reaction of CO with nonpolar probes (**16a−c**, **19**, **20**) in PBS (using various amounts of organic cosolvents, such as dimethylsulfoxide (DMSO), tetrahydrofuran (THF), acetonitrile, 10−50%) was inhibited probably because of a large amount of coordinating organic cosolvent, and the formation of many side products was observed. Still, reduction was the major reaction pathway (Scheme 9).

Interaction of Sensors with Mouse Hepatoma Cells. To select a few derivatives for spectroscopic and kinetic studies, the interaction of cells with a CO sensor was evaluated following the exposure of mouse hepatoma (Hepa 1−6) cells to Nile red probes without (**16b**) and with water-solubilizing sulfonic (**17b**, **18b**) groups. After incubation, the cells were washed with PBS and visualized under a fluorescence microscope. Intensive fluorescence was detected after treating Hepa 1−6 cells only with **16b**, whereas almost no signal and only a distinct plasma membrane fluorescence following treatment with **17b** and **18b** were observed, respectively, indicating a limited penetration of **17b** and **18b** into the intracellular compartment (Figure S89). As a result, less polar derivatives were selected for further experiments. It has been reported that Pd^{II} ion inhibits enzyme activities at concentrations ranging from 20 to 500 mmol L^{-1}, attributed to the binding of Pd^{II} to enzymes, which leads to an altered peptide conformation and destruction of catalytic activity.[63] For example, cellular function inhibition occurs at 100−400 mmol L^{-1}, whereas DNA synthesis is inhibited at 100−300 mmol L^{-1}.[64] As the concentration of our sensor (10 μM) is much lower than that in the studied systems, and most importantly, any apparent toxicity of the sensor was not observed in any our studies under our experimental conditions, we assumed that toxicity of Pd^{II} does not interfere with our results.

Optical Properties of Nile Red Derivatives and Palladacycles. Nile red is a solvatochromic dye,[65] and its absorption and emission maxima and fluorescence quantum yields are considerably affected by solvent polarity. Its absorption and emission maxima exhibit strong bathochromic shifts[66] in polar solvents, whereas the fluorescence quantum yield decreases with an increased hydrogen-bonding power.[67] A low fluorescence quantum yield in water is also attributed to the H-type aggregation of the dye as a consequence of its low solubility.[68]

The absorption and emission maxima and fluorescence quantum yields of palladacycles **16a−c** and **20** and Nile red derivatives **12−15** and **21a** (the products of CO reaction) are summarized in Table 2 (see also Figures S59−S64). The

Table 2. Photophysical Properties of Nile Red Derivatives and Palladacycles in Methanol

compd	ε_{max}[a] (10^4 dm^3 mol^{-1} cm^{-1})	λ_{max}(abs) (nm)	λ_{max}(em) (nm)[b]	Φ_F[e]
12a	4.2	553	640	0.51, (0.38),[72] (0.40)[67]
12b	4.2	547	637	0.50, (0.47)[73]
12c	1.2	557	643	0.44
12e	3.3	560	647	0.46
13a	3.0, 3.3[c]	552, 564[c]	640, 659[c]	0.44, 0.063,[c] 0.091[d]
13b	3.0, 2.6[c]	549, 560[c]	637, 655[c]	0.54, 0.097,[c] 0.10[d]
14a	2.4, 2.6[c]	552, 571[c]	640, 654[c]	0.55, 0.19,[c] 0.20[d]
14b	2.0, 2.7[c]	546, 561[c]	637, 652[c]	0.60, 0.13,[c] 0.20[d]
15	4.4	552	649	0.49
16a	3.8[h]	610[h]	715[h]	0.080[h]
16b	3.4[h]	610,[h] 608[f]	718,[h] nd[f,g]	0.010,[h] nd[f,g]
16c	3.3[h]	630[h]	717[h]	0.065[h]
20	2.5[h]	616[h]	716[h]	0.080[h]
21a	4.0	561	635	0.54

[a]The values ε for palladacycles were calculated using the molar masses of the dimers. [b]λ_{ex} (palladacycles **16a−c**, **20**) = 600 nm, λ_{ex} (Nile red derivatives) = 520 nm. [c]In PBS (pH = 7.4, 10 mM, I = 0.1 M). [d]In water. [e]Φ_F was determined in solutions with $A(\lambda_{ex}) < 0.1$; the values in parentheses were taken from the literature. [f]In PBS (pH = 7.4, 10 mM, I = 0.1 M) with 5% DMSO. [g]nd = no fluorescence detected. [h]In a methanol/dichloromethane mixture (9:1).

https://dx.doi.org/10.1021/acs.joc.9b03217
J. Org. Chem. XXXX, XXX, XXX−XXX

absorption and emission maxima of Nile red derivatives and palladacycles in methanol were found not to be significantly influenced by the substituents. The fluorescence quantum yields of all Nile red derivatives in methanol were comparable (0.45−0.55), whereas those of palladacycles were low due to the quenching by a heavy atom (Pd).[69] The fluorescence quantum yield of 2-hydroxy derivative **16b** (0.01) is almost an order of magnitude lower than that of the other derivatives, which is very important when this system is considered as a potential chemosensor (the background initial fluorescence of an off−on sensor should be as low as possible). Interestingly, some reported Nile red Pd complexes exhibited high fluorescence quantum yields (~0.5), which was attributed to the low-energy ligand-centered excited states that are not influenced by nonemissive metal-centered excited states.[70,71] The absorption and emission maxima of all compounds in PBS were bathochromically shifted compared to those in methanol (Table 2). The fluorescence quantum yields of water-soluble derivatives (**13a,b**, **14a,b**) increased with the number of solubilizing groups attached to the molecule, which can be explained by the presence of charged sulfonic groups that make the compounds less predisposed to aggregation.[72]

Thermal Stability and Photostability. Sensors **16a−c** and **20** are not stable in methanol in the dark. They slowly decompose to give the corresponding Nile red derivatives, that is, the products of reduction (see the Experimental Section). The rate of **16b** decomposition at room temperature was 9.7×10^{-6} s^{-1}; thus, the half-life of the sensor in this solvent was ~20 h (Figure S65). The thermal stability and photostability of palladacycle **20** (c = 10 mM) were also examined in PBS (5% DMSO) by emission spectroscopy. The compound was found to be stable for 8 h in the dark (Figure S66); however, it degrades photochemically under aerobic conditions. Irradiation of the sample (**20**, 10 μM, 5% DMSO in PBS) with 590 nm light-emitting diodes (LEDs) led to a 3-fold fluorescence enhancement over 4 h until the signal leveled off, suggesting that singlet oxygen, which can be generated by triplet−triplet annihilation of triplet-excited **20** with ground-state oxygen, might be responsible for the conversion of the palladacycle into a fluorescent Nile red derivative. In contrast, compound **20** was found to be sufficiently photostable under anaerobic conditions.

Reaction Kinetics of CO Sensing. The course of the reaction of palladacycles with CO was first studied by absorption spectroscopy under pseudo-first-order conditions with an excess of CO (CO atmosphere) and a nucleophile (methanol). The absorption spectra changes during the reaction of derivatives **16a−c** with CO are shown in Figure 2, where the spectra in red are always assigned to an initial palladacycle. After a methanolic solution was purged with pure CO, the formation of an intermediate (green line) was observed within a few seconds. Thus, this first step must be very fast, whereas the subsequent transformation of these intermediates to the final methyl ester products (blue spectrum) is considerably slower.

The recorded kinetic data related to the transformation of an intermediate to the product were subjected to target analysis. Singular value decomposition (SVD)[74] of the kinetic data was performed to distinguish the number of individual species involved. We concluded from the magnitude of singular values (Figure S83) and shapes of the spectral and trace vectors that there are two contributing components in the case of derivatives **16a−c**. A simple A → B kinetic model with one

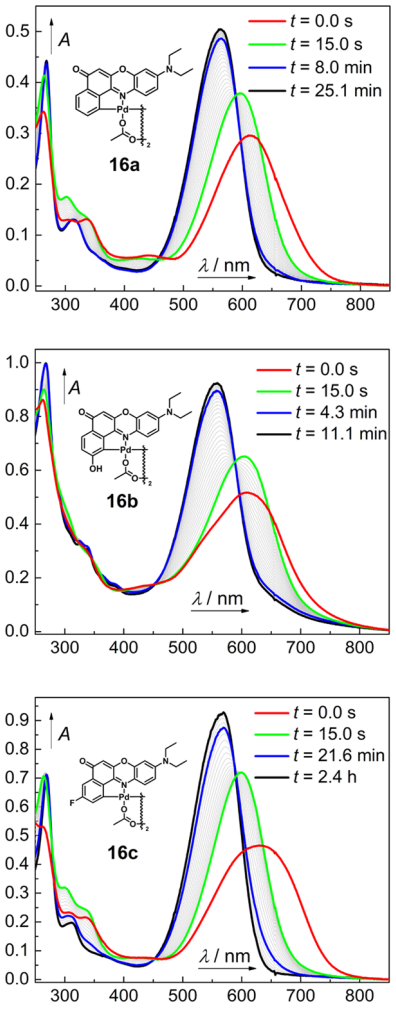

Figure 2. Reactions of palladacycles (c ~ 10 μM) under the CO atmosphere in methanol studied by absorption spectroscopy at 20.0 °C.

rate constant (first order) was used to fit the data (Table 3). The kinetics of trifluoroacetate-bridged palladacycle **20** cannot be directly compared to the other derivatives because the simultaneous formation of methyl ester **21a** and a reduction product **12a** was observed. A branching model was used for fitting (see Figures S87 and S88).

Table 3. Kinetic Data for the Rate-Determining Step in the Reaction of Nile Red Palladacycles in Methanol under CO Atmosphere[a]

compd	k_{AB} (10^{-3} s^{-1})	τ_{AB} (min)
16a	7.3 ± 0.2	2.3 ± 0.1
16b	13.0 ± 0.5	1.3 ± 0.1
16c	1.24 ± 0.05	13.4 ± 0.5

[a]The rate constants were obtained by target analysis using spectroscopic data from the reactions of palladacycles (c ~ 10 μM) with CO (1 atm) in methanol at 20.0 ± 0.1 °C. An A → B kinetic model was used in all cases.

To unravel the structure of a long-lived intermediate, we performed the same experiment with palladacycle **16a**, but the solution was purged with argon after CO addition (Figure 3). A slow disappearance of the absorption band of an intermediate at 596 nm and the appearance of a band that

https://dx.doi.org/10.1021/acs.joc.9b03217
J. Org. Chem. XXXX, XXX, XXX−XXX

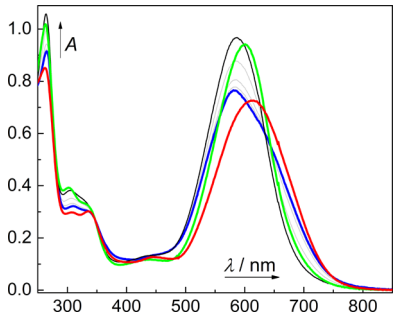

Figure 3. Reversible binding of CO to **16a** in methanol. A solution of **16a** (thick red line) was purged with CO for 15 s (thick green line); it was allowed to react for 30 s (black line) and then purged with argon (gray lines) for 4 min (thick blue line).

corresponds to the initial complex (at 613 nm) were observed upon excessive argon purging, suggesting that CO binding occurs in the first step and is reversible. Because the reaction was conducted in methanol, we also detected the formation of methyl ester **21a** during purging the solution with argon. The final spectrum (after 4 min of argon purging) can be expressed as a linear combination of the spectra of starting material **16a** and product **21a** (Figure S78).

A reversible binding of CO in a dichloromethane solution was also observed for trifluoroacetate-bridged complex **20** (Figure S76) but not for acetate-bridged palladacycles **16a–c**. This finding is in accordance with the bridge-splitting equilibrium constants found for pyridine (Table 1), where the derivative **20** reacted with pyridine quantitatively, but a large excess was necessary in the case of acetate derivatives **16a–c** (trifluoroacetate is a better leaving group than acetate). Ligand exchange of CO by pyridine in complex **20** was monitored by UV–vis spectroscopy, and the species involved were directly detected by ESI-MS. In addition, the collision-induced dissociation (CID) of a mixed pyridine/CO-coordinated complex (**12a**-H)$_2$Pd$_2$(pyridine)(CF_3COO^-)(CO) led to the loss of CO (Figure S77).

To get a deeper insight into the reaction mechanism, we attempted to identify the reaction intermediates observed in spectroscopic experiments (Figure 2) by ESI-MS.[75] No species were detected under these conditions, most probably because of their poor stability even under soft ionization conditions.[76] However, the addition of pyridine led to the formation of detectable complexes. For example, the reaction of complex **16a** gave a mixed CO/pyridine adduct along with the formation of the final carbonylation product **21a** (Figure S79). Therefore, we assign the intermediates (green spectrum, Figure 2) to the CO-coordinated complex according to the following considerations: (a) The CO binding is reversible in both methanol (Figure 3) and dichloromethane (Figure S76); (b) CO/pyridine adducts were detected by ESI-MS, and they release CO under the CID experiments (Figures S77 and S79); and (c) no other reaction intermediates were detected.

This reaction mechanism was also studied by NMR. The addition of dichloromethane-d_2 as an inert cosolvent was necessary for dissolving larger amounts of the starting material, and it had no effect on the product formation. Unfortunately, only the decay of palladacycle **16a** to give product **21a** was observed (Figure S57). The explanation is trivial; the solubility of CO in methanol ($\sim 10^{-2}$ M)[77] is sufficient to convert starting palladacycle to a CO-coordinated intermediate at low concentrations used in spectroscopic experiments but not at 2 orders of magnitude higher concentrations in an NMR tube.

In addition, the reaction kinetics of **16a–c** and **20** ($c \sim 1$ μM) in methanol under a CO atmosphere was studied by emission spectroscopy. The fluorescence enhancement due to the formation of fluorescent products are usually calculated from the time-dependent emission spectra (Figure 4a) as the

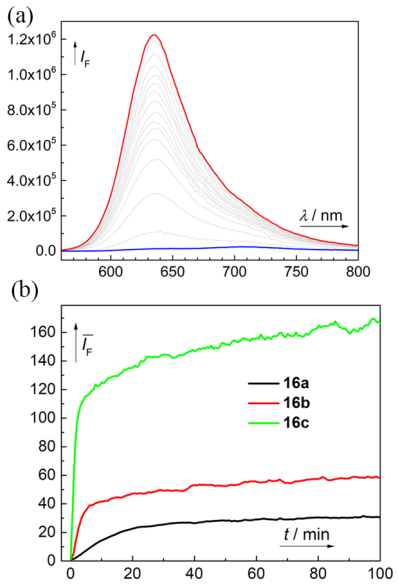

Figure 4. (a) Representative time-dependent emission spectra of the reaction of **16a** ($c \sim 1$ μM, λ_{ex} = 520 nm; measured for ~2 h) under CO atmosphere in methanol. (b) Time evolution of $\bar{I}_F$ for **16a–c**.

ratio of fluorescence intensities at the corresponding wavelengths (typically emission maxima).[38−41] In this work, complete spectra were used in the calculation to improve the signal-to-noise ratio (eq 1) and to clearly distinguish the signals of the initial and end states. The fluorescence enhancement ($\bar{I}_F$) is proportional to the ratio of the fluorescence quantum yields of the starting palladacycle and the product; thus, the lower the fluorescence quantum yield of palladacycle, the higher the fluorescence enhancement.

$$\bar{I}_F = \frac{\int_{\lambda_1}^{\lambda_2} I_F(\lambda, t)\mathrm{d}\lambda}{\int_{\lambda_1}^{\lambda_2} I_F(\lambda, 0)\mathrm{d}\lambda} \propto \frac{\Phi_{F,p} \times \varepsilon_p(\lambda_{ex})}{\Phi_{F,c} \times \varepsilon_c(\lambda_{ex})} \quad (1)$$

where $I_F(\lambda,t)$ is the fluorescence intensity at time t and wavelength λ; $\Phi_{F,p}$ and $\Phi_{F,c}$ are the fluorescence quantum yields of the product and the corresponding complex, respectively; and $\varepsilon_p(\lambda_{ex})$ and $\varepsilon_c(\lambda_{ex})$ are the molar absorption coefficients at the excitation wavelength of the related species.

Our results show that **16b** exhibits a much greater fluorescence enhancement than $\bar{I}_F$ of the other derivatives (Figure 4b), which is simply related to a very low fluorescence quantum yield of the starting compound **16b** (Φ_F = 0.01 in methanol; Table 2), being responsible for a lower signal-to-noise ratio, whereas Φ_F of **21a** is comparable to Φ_F's of other Nile red derivatives listed in Table 2. The rate of CO sensing followed the trend of **16b** > **16a** > **16c** (Table 3). The electron-donating hydroxyl group (**16b**) increased and the electron-withdrawing fluoride (**16c**) decreased the reaction rate by factors of approximately 1.8 and 6, respectively, compared to that of an unsubstituted derivative **16a** (Table 3).

https://dx.doi.org/10.1021/acs.joc.9b03217
J. Org. Chem. XXXX, XXX, XXX−XXX

Scheme 10. Proposed Mechanism of CO Sensing in Methanol

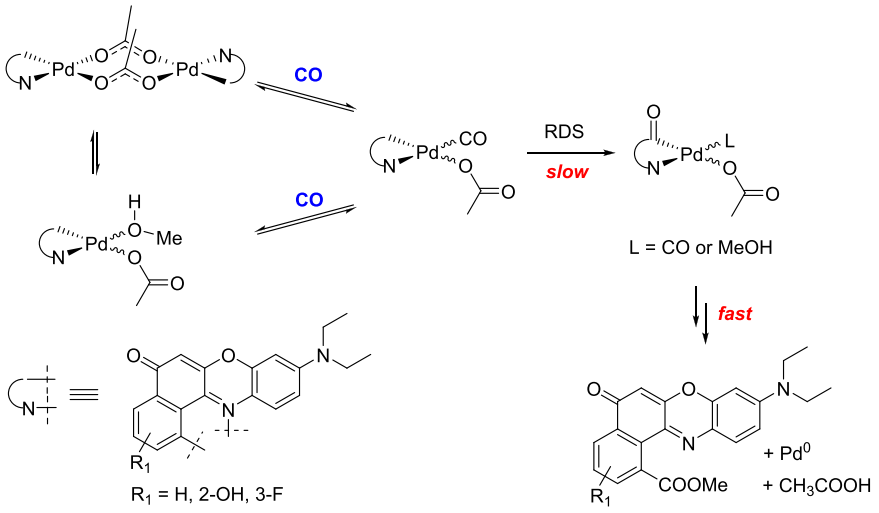

Reaction Mechanism. Our experiments provided evidence that the CO coordination is a reversible but rapid reaction step to give a long-lived carbonyl complex as an intermediate. No other reaction intermediate was detected or indicated in our kinetic spectroscopic experiments. Therefore, the subsequent process must be rate-determining, followed by rapid reaction steps to give the final products. If a CO insertion into palladacycles is the rate-determining step (Scheme 10), the reaction should be sensitive to the nature of the migrating group. It has been shown that electron-donating groups accelerate CO insertion into palladacycles and vice versa.[78] We observed the same trend, and we propose that the CO insertion is the rate-determining step (Table 3). Therefore, the sensing mechanism most likely involves CO coordination, CO insertion, and the subsequent reductive elimination steps (Scheme 10).

The overall fluorescence enhancement $\overline{I}_F$ is the major feature for sensing applications where the detection sensitivity is a key issue. Incomparably, the greatest $\overline{I}_F$ was found for the derivative **16b** (Figure 3), considerably exceeding the sensitivity of a nonsubstituted derivative **16a** reported earlier.[40] As this sensing process is also the fastest, **16b** represented the best candidate for the subsequent biological studies.

Biological Experiments. A biological usability of CO sensing was investigated with sensor **16b** (10 μM) in the cell culture of mouse hepatoma (Hepa 1−6) cells after incubation in the presence of a photoactivatable CO-releasing molecule (photoCORM; 4,8-dimethoxy-6,6-dimethyldibenzo[*b*,*f*]-cyclopropa[*d*]silepin-1(6*H*)-one), which activates CO production upon irradiation.[79] The cells were washed with PBS after reaching an 80% confluence and were incubated with increasing concentrations of photoCORM. After activation of CO release upon irradiation at 400 nm, followed by 15 min incubation in the dark, the fluorescence intensity was determined using a microplate reader, and the samples were visualized by fluorescence microscopy. A linear increase in the fluorescence was observed in the photoCORM concentration range of 60−1000 μM (Figure 5). These data were in concordance with live-cell CO imaging using fluorescence microscopy, where a substantial CO-dependent increase in the fluorescence intensity and intracellular accumulation of **16b** were observed (Figure 6). In this set of experiments, the probe concentration as well as the exposure time during imaging remained constant to clearly demonstrate the relationship between fluorescence intensity and CO concentration.

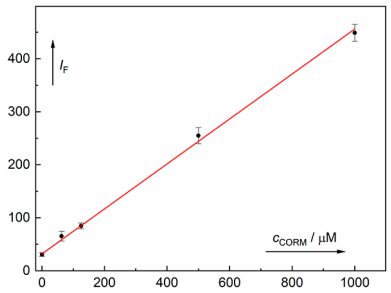

Figure 5. Fluorescence intensity increase of **16b** (λ_{ex} = 530 nm, λ_{em} = 645 nm) in the presence of CO released from a photoCORM at concentrations of 62.5, 125, 500, and 1000 μM after 5 min irradiation with an LED source (400 nm) in Hepa 1−6 cells on a microplate reader. The values represent mean ± SD (n = 8).

CONCLUSIONS

Differently substituted Nile red palladacycles with core and bridging ligand modifications were synthesized as CO fluorescent off−on sensors in aqueous solutions. We determined their optical properties and reactivities with CO using time-dependent absorption and fluorescence spectroscopies. The longest-living intermediate in CO sensing was found to be a CO-coordinated complex, followed by CO insertion as the rate-determining step. An electron-donating core substituent in **16b** was found to increase the overall reaction rate and the overall fluorescence enhancement. The sensing reaction of this compound was then successfully tested in biological samples using fluorescence microscopy, which enabled in situ visualization and localization of metabolic processes employing CO within the specific cellular and subcellular compartments. From this perspective, the sensor **16b** represents a very promising molecule easily crossing the plasma membrane and qualitatively tracing the localization of CO within the cell interior with the linear quantitative response to increasing CO concentrations. Further in vitro and in vivo studies are needed to uncover the whole biological potential of this probe.

https://dx.doi.org/10.1021/acs.joc.9b03217
J. Org. Chem. XXXX, XXX, XXX−XXX

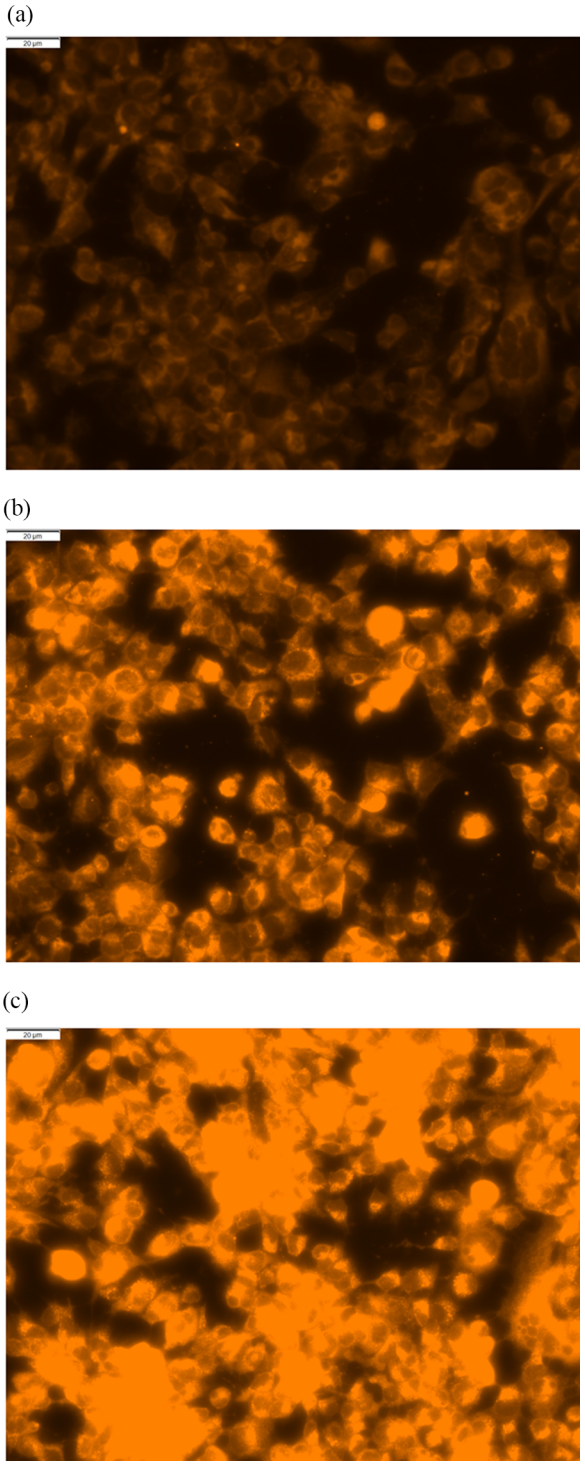

Figure 6. Fluorescence microscopy images of **16b** with increasing concentrations of CO (62.5, 500, and 1000 μM (a–c); see the footnotes in Figure 5) in Hepa 1–6 cells at fixed exposure times. The scale bars represent 20 μm.

EXPERIMENTAL SECTION

Materials and Methods. Melting points were measured on a noncalibrated Kofler's hot-stage melting-point apparatus. NMR spectra were obtained on 75 and 126 MHz (^{13}C), and 300 and 500 MHz (^{1}H) spectrometers in chloroform-*d*, dimethylsulfoxide-d_6, methanol-d_4, water-d_2, and dichloromethane-d_2, and they were referenced to the residual peak of the (major) solvent except for those of ^{19}F NMR. All NMR measurements were conducted at 30 °C. IR spectra were recorded on a Fourier transform spectrometer using solid samples. HRMS spectra were obtained on a triple-quadrupole ESI mass spectrometer in a positive and/or negative mode. UV–vis spectra were measured in 10.0 mm quartz fluorescence cuvettes using a UV–vis spectrometer. Emission spectra were recorded on a luminescence spectrometer in 10.0 mm quartz fluorescence cuvettes. HPLC (C-18 column) analysis was performed by gradient elution (50:50 to 0:100 of solutions *A*:*B*, where *A* = 0.1 M NH_4OAc in H_2O and *B* = 0.1 M NH_4OAc in methanol). All column chromatography procedures were performed on columns packed with silica gel (63–200 μm). Thin-layer chromatography (TLC) was performed using silica gel plates (0.2 mm thickness) and visualized under a UV lamp (254 nm, 366 nm). All solvents and chemicals were used as purchased or purified/dried by standard procedures when necessary. Unless otherwise specified, all procedures were carried out under a nitrogen atmosphere. Reaction mixtures were heated using a hot plate with magnetic stirring in an oil bath.

Determination of Fluorescence Quantum Yields. Fluorescence quantum yields were determined as the absolute values using an integration sphere. The quantum yields were measured three times and then averaged for each sample. The concentrations of the solutions were kept low ($A < 0.1$). The fluorescence quantum yields were determined in methanol, PBS (pH = 7.4, 10 mM, I = 0.1 M), or water. The 520 nm excitation wavelength was used for the determination of the fluorescence quantum yields of Nile red derivatives (**12a–c**, **12e**, **13–15**), and the 600 nm excitation wavelength was used for Nile red-derived palladacycles (**16a–c**, **20**). The wavelength of 600 nm was chosen to eliminate the effect of ubiquitous impurities of Nile red derivatives, whose molar absorption coefficient at 600 nm is sufficiently small.

Determination of Bridge-Splitting Equilibrium Constant. Two solutions of the same concentrations (~10 μM) of palladacycles **16a–c** or **20** in dry dichloromethane were prepared, and the corresponding amount of pyridine was added to one of them. The solution of a pure palladacycle was then titrated with the other solution, and absorption spectra were recorded upon each addition. The pyridine concentration-dependent spectra were then subjected to global fitting using the corresponding equilibrium model (Supporting Information, page S79; Figures S80–S82).

Reaction Kinetics of Nile Red Palladacycles (16a–c, 20) with CO in Methanol. All solutions were freshly prepared before the measurements. The palladacycles decompose over time in both DMSO and methanol (see below).

Absorption Spectroscopy. A solution (~10 μM) of Nile red palladacycle (**16a–c**, **20**) in methanol was prepared by dissolving the pure compound in a drop of dry dichloromethane (~0.1 mL) and dilution with dry methanol. This solution was then filtered through a syringe filter prior to each measurement to remove any undissolved solids. A filtered solution (2 mL) was added to a cuvette (total volume, 4.6 mL) equipped with a stir bar and silicon septum. The cuvette was inserted into a spectrometer, and the solution was stirred. The absorption spectrum before the addition of CO was recorded, and subsequently, the solution was purged with pure CO for 15 s while the air was vented out via another syringe. Both syringes were removed and time-dependent absorption spectra were recorded in a thermostated cuvette holder setup at 20.0 ± 0.1 °C for ~ 2 h under stirring.

Emission Spectroscopy. A stock solution of palladacycle (**16a–c**) was prepared in the same manner as that for the absorption kinetic measurements. An ~1 μM solution ($A < 0.1$) was prepared from the stock solution by dilution, and one part (2 mL) was added to a cuvette (total volume, 4.6 mL) equipped with a stir bar and a silicon septum. The cuvette was placed into a fluorimeter and equipped with a magnetic stirrer. CO was introduced to a solution in the same manner as was described in the case of absorption spectra measurements. Time-dependent emission spectra (560–800 nm) were recorded every 30 s (dwell time, 0.08 s; 2 nm step; one repeat) for ~2 h with the excitation wavelength of 520 nm at room temperature.

https://dx.doi.org/10.1021/acs.joc.9b03217
J. Org. Chem. XXXX, XXX, XXX–XXX

Thermal Stabilities in Methanol and Rates of Decomposition. A solution of **16a** (~5 mg) in methanol (20 mL) was refluxed under an air atmosphere for 16 h. Palladium black was formed in the course of the reaction as a black precipitate. The suspension was filtered through a pad of Celite and evaporated. The crude residue was analyzed by ^{1}H NMR. The formation of the parent Nile red (**12a**) along with acetic acid was evident by ^{1}H NMR.

The rate of thermal decomposition of **16b** in methanol was studied by time-dependent fluorescence spectroscopy. The solution of **16b** in methanol (c ~ 20 μM) was prepared and transferred to a fluorescent cuvette equipped with a septum. Time-dependent fluorescence spectra (dwell time, 0.2 s; 1 nm step, two repeats) were measured every ~10 min over the course of 16 h at room temperature with an excitation wavelength of 520 nm (Figure S65a). The decomposition rate constant was determined from the concentration change of the product **12b** (at 630 nm; Figure S65b).

Thermal Stability and Photostability in PBS. A solution of compound **20** (10 μM) in PBS (5% DMSO, 10 mM, I = 0.1 M) in a capped cuvette equipped with a silicon septum was irradiated by 590 nm LEDs in a cuvette holder for 8 h. The emission spectra were taken every 1 h (Figure S66). For deoxygenated conditions, the same experiment was performed, but the solution of the complex was purged with argon for 1 min before the irradiation started (Figure S66).

NMR Kinetics. A solution of **16a** (3.4 mg) in CD_3OD/CD_2Cl_2 (0.6 mL, 4:2, v/v) was prepared in an NMR tube. The air above the solution was exchanged by a pure CO atmosphere, and the solution was shaken. Time-dependent ^{1}H NMR spectra were then acquired (Figure S57).

Biological Experiments. Hepa 1−6 mouse hepatoma cell line (ATCC CRL-1830) was grown in 48-well plates according to the manufacturer's instructions. The cells were kept at 37 °C and 5% CO_2 atmosphere throughout the experiment. Fluorescence was measured using a multidetection microplate reader at λ_{ex} = 530 nm and λ_{em}= 645 nm, and the cells were visualized under a fluorescence microscope (emission filter: 420 nm). The pictures were taken under a constant exposure time of 100 ms.

Global Fitting. Different data (either time-resolved spectroscopic data from the kinetic measurements or concentration-dependent spectroscopic data from the determination of equilibrium constants), represented by a matrix $\mathbf{D} = \mathbf{CS}^T + \mathbf{E}$, were decomposed into the concentration $\mathbf{C}$ and spectra $\mathbf{S}^T$ matrices with an error $\mathbf{E}$ by a variable projection approach.[80] The corresponding kinetic or equilibrium model with nonlinear parameters $\boldsymbol{\Theta}$ was applied as a model for the calculation of the concentration matrix $\mathbf{C} = \mathbf{C}(\boldsymbol{\Theta})$. The spectra matrix $\mathbf{S}^T$ is conditionally linear ($\mathbf{S}^T = \mathbf{C}^+\mathbf{D}$) on $\mathbf{C}$, where $\mathbf{C}^+ = (\mathbf{C}^T\mathbf{C})^{-1}\mathbf{C}^T$ is the Moore−Penrose pseudoinverse. Minimization of the sum of squares of residuals $\|\mathbf{CS}^T - \mathbf{D}\|_2^2 = \|(\mathbf{CC}^+ - \mathbf{I})\mathbf{D}\|_2^2$ for the parameters defined in a corresponding model by the Levenberg−Marquardt algorithm provided the best fit of $\mathbf{C}$ and $\mathbf{S}^T$ with optimized parameters. Routines for the fitting were programmed with the use of an LMFIT package.[81]

ESI-MS Experiments. The experiments were performed with an ion-trap mass spectrometer equipped with an HESI source operating in the positive mode.[82] The palladacycles were diluted by a solvent (methanol or dichloromethane containing traces of pyridine) to the corresponding concentration of 5 × 10^{-5} M and were introduced to an HESI source at a rate of 3 μL min^{-1}. The operating conditions were set as follows: spray voltage, 3.7 kV; capillary voltage, 3 V; tube lens offset, 119 V; and heated capillary temperature, 150 °C. All of the mass spectra were recorded from m/z 50 to 2000.

Synthesis. *6-Fluoro-1,4-dihydro-1,4-epoxynaphthalene (**1**).* The compound was prepared according to a known procedure.[52] A suspension of furan (2.0 equiv, 7.5 mL, 104 mmol) and Mg turnings (1.64 g, 67.4 mmol) in dry THF (80 mL) was prepared and heated to 60 °C. The Mg turnings were activated by the addition of iodine (~20 mg) to the mixture. A solution of 1-bromo-2,4-diflourobenzene (10.0 g, 51.8 mmol) in dry THF (25 mL) was added dropwise to the prepared mixture at a rate to maintain the suspension at a gentle reflux (~30 min). The reaction mixture was then stirred at 65 °C for 15 h. After cooling to room temperature, the mixture was filtered through a pad of Celite, and the filtrate was concentrated on a rotary evaporator to a volume of ~30 mL. The mixture was quenched with water (30 mL) and extracted with diethyl ether (3 × 50 mL); brine (30 mL) was added to facilitate separation of the layers. The organic extracts were combined, dried over anhydrous $MgSO_4$, and evaporated under reduced pressure to afford the title compound as an amber oil, which was subsequently used in the next step without further purification. Yield 7.00 g (83%). ^{1}H NMR (300 MHz, $CDCl_3$): δ (ppm) 7.14 (dd, J = 7.8, 4.6 Hz, 1H), 7.08−6.96 (m, 3H), 6.63 (ddd, J = 9.8, 7.8, 2.3 Hz, 1H), 5.69 (s, 2H). ^{19}F NMR (282 MHz, $CDCl_3$): δ (ppm) −117.66 (ddd, J = 9.7, 7.7, 4.6 Hz, 1F). The spectroscopic data are consistent with those reported in the literature.[83]

*7-Fluoronaphthalen-1-ol (**2**).* The compound was prepared according to a known procedure.[52] Diethyl ether·BF_3 (5.6 mL, 45.3 mmol) was added dropwise to a solution of crude 6-fluoro-1,4-dihydro-1,4-epoxynaphthalene (**1**, 7.00 g, 43.2 mmol) in dry dichloromethane (90 mL) at 0 °C. After this addition (30 min), the mixture was allowed to warm to room temperature and then stirred for additional 2 h. The resulting solution (dark brown) was washed with water (3 × 80 mL). The organic layer was separated, dried with anhydrous Na_2SO_4, and the solvent was evaporated under reduced pressure to yield a dark orange crystalline mass. The mixture was chromatographed first with dichloromethane/hexane (1:1, v/v) and then with dichloromethane as a mobile phase to yield the mixture of 7- and 6-fluoro (**3**) isomers, in the ratio of ~14:1 (from integration of signals in ^{19}F NMR spectrum). The solid was then recrystallized from boiling chloroform to produce crystals, which were filtered and washed with hexane (10 mL) to yield a white cotton candy-looking crystals with a characteristic naphthol aroma. Yield 3.10 g (44%). ^{1}H NMR (300 MHz, $CDCl_3$): δ (ppm) 7.86−7.75 (m, 2H), 7.44 (d, J = 8.3 Hz, 1H), 7.34−7.21 (m, 2H), 6.83 (d, J = 7.5 Hz, 1H), 5.16 (s, 1H). ^{19}F NMR (282 MHz, $CDCl_3$): δ (ppm) −114.66 (ddd, J = 10.3, 8.5, 5.6 Hz, 1F). ^{13}C{^{1}H} NMR (75 MHz, $CDCl_3$): δ (ppm) 160.6 (d, $^1J_{C-F}$ = 245.1 Hz), 151.1 (d, J_{C-F} = 5.4 Hz), 132.0, 130.2 (d, J_{C-F} = 8.8 Hz), 125.3 (d, J_{C-F} = 9.0 Hz), 125.1 (d, J_{C-F} = 2.5 Hz), 120.8 (d, J_{C-F} = 1.1 Hz), 117.0 (d, J_{C-F} = 25.4 Hz), 109.5, 105.8 (d, J_{C-F} = 22.3 Hz). The spectroscopic data are consistent with those reported in the literature.[52]

*1H-Naphtho[1,8-de][1,2,3]triazine (**4**).* The compound was prepared according to a known procedure.[53] A solution of $NaNO_2$ (1.05 equiv, 4.72 g, 68.4 mmol) in water (27 mL) was added to a solution of naphthalene-1,8-diamine (10.3 g, 65.1 mmol) in a mixture of acetic acid (120 mL) and water (90 mL) at −6 °C under vigorous stirring. The reaction temperature was raised to 10 °C; then, the reaction mixture was diluted with water (30 mL) and stirred at 0 °C for another 45 min. The brown precipitate was filtered off, washed with water (30 mL), and dried at room temperature to give a fine red-brown powder, which was a sufficiently pure title compound for the next step. Yield 10.0 g (91%). ^{1}H NMR (300 MHz, DMSO-d_6): δ (ppm) 13.15 (bs, 1H), 7.31−7.05 (m, 4H), 6.52 (d, J = 5.7 Hz, 2H). ^{13}C{^{1}H} NMR (75 MHz, DSMO-d_6): δ (ppm) 136.0, 133.5, 129.1, 120.8, 118.4, 106.2 (bs). HRMS (APCI$^-$) m/z: [M − H]$^-$ calcd for $C_{10}H_6N_3$ 168.0567; found 168.0566. The spectroscopic data are consistent with those reported in the literature.[53]

*8-Fluoronaphthalen-1-amine (**5**).* The compound was prepared according to a known procedure.[54] 1*H*-Naphtho[1,8-*de*][1,2,3]-triazine (**4**, 3.38 g, 20.0 mmol) was added slowly in portions to a solution of hydrogen fluoride/pyridine (70% HF in pyridine, 33 equiv, 17 mL, 654 mmol) in a HD-PE flask with magnetic stirring while cooling in an ice bath. The reaction flask was capped with a septum, and a balloon with nitrogen was attached. The reaction solution was stirred at room temperature for 7 days. The diluted reaction mixture with water (100 mL) and ice (50 g) was neutralized with an ice-cold solution of KOH (44.8 g, 799 mmol) in water (200 mL) while cooling in an ice bath. The solution was then extracted with ethyl acetate (4 × 70 mL). The extracts were combined and washed with brine (50 mL), dried using anhydrous Na_2SO_4, and evaporated under reduced pressure to yield crude naphthylamine. It was purified by column chromatography with dichloromethane as a

https://dx.doi.org/10.1021/acs.joc.9b03217
J. Org. Chem. XXXX, XXX, XXX−XXX

mobile phase to give a pink solid. Yield 1.60 g (50%). ^{1}H NMR (300 MHz, $CDCl_3$): δ (ppm) 7.52 (dd, J = 8.3, 0.9 Hz, 1H), 7.38−7.17 (m, 3H), 6.99 (ddd, J = 14.8, 7.6, 1.1 Hz, 1H), 6.67 (dd, J = 7.3, 1.2 Hz, 1H), 4.79 (s, 2H). ^{19}F NMR (282 MHz, $CDCl_3$): δ (ppm) −116.06 (ddd, J = 14.7, 5.3, 2.4 Hz, 1H). ^{13}C{^{1}H} NMR (75 MHz, $CDCl_3$): δ (ppm) 160.5 (d, $^1J_{C-F}$ = 247.9 Hz), 142.6 (d, J_{C-F} = 3.4 Hz), 137.4 (d, J_{C-F} = 4.5 Hz), 127.8 (d, J_{C-F} = 1.6 Hz), 125.6 (d, J_{C-F} = 10.0 Hz), 124.6 (d, J_{C-F} = 3.9 Hz), 117.3 (d, J_{C-F} = 3.2 Hz), 113.6 (d, J_{C-F} = 10.0 Hz), 110.2 (d, J_{C-F} = 2.0 Hz), 109.3 (d, J_{C-F} = 23.9 Hz). HRMS (APCI$^+$) m/z: $[M + H]^+$ calcd for $C_{10}H_9FN$ 162.0714; found 162.0714. The spectral data are consistent with those reported in the literature.[54]

*8-Fluoronaphthalen-1-ol (**6**).* A solution of $NaNO_2$ (0.276 g, 4.00 mmol) in water (5 mL) was added dropwise to an ice-cooled suspension of 8-fluoronaphthalen-1-amine (**5**, 0.580 g, 3.60 mmol) in a solution of concn H_2SO_4 (98.0%, 4.6 mL, 84.9 mmol) in water (30 mL) under nitrogen atmosphere. The reaction mixture was stirred for 20 min at room temperature and then steam-distilled (excess of water was added to the reaction mixture, 100 mL) under a nitrogen atmosphere until no product appeared. The product was washed from a condenser with ethyl acetate, and the distillate was extracted with ethyl acetate (2 × 30 mL). Washings and extracts were combined, washed with brine (30 mL), dried under anhydrous $MgSO_4$, and evaporated to afford pale yellow crystals. Yield 0.365 g (63%). ^{1}H NMR (300 MHz, $CDCl_3$): δ (ppm) 7.62 (dd, J = 8.3, 1.0 Hz, 1H), 7.45−7.39 (m, 2H), 7.35 (td, J = 8.0, 5.7 Hz, 1H), 7.09 (ddd, J = 15.1, 7.7, 1.0 Hz, 1H), 7.03−6.95 (m, 1.5H), 6.91 (s, 0.5H). ^{19}F NMR (282 MHz, $CDCl_3$): δ (ppm) −121.39 (ddd, J = 26.5, 15.0, 5.3 Hz, 1H). ^{13}C{^{1}H} NMR (75 MHz, $CDCl_3$): δ (ppm) 159.5 (d, $^1J_{C-F}$ = 242.3 Hz), 151.6 (d, J_{C-F} = 1.1 Hz), 137.2 (d, J_{C-F} = 3.5 Hz), 128.1 (d, J_{C-F} = 1.5 Hz), 125.7 (d, J_{C-F} = 10.1 Hz), 124.9 (d, J_{C-F} = 3.7 Hz), 119.8 (d, J_{C-F} = 3.2 Hz), 113.9 (d, J_{C-F} = 7.3 Hz), 111.6 (d, J_{C-F} = 2.6 Hz), 109.7 (d, J_{C-F} = 22.8 Hz). HRMS (APCI$^-$) m/z: $[M - H]^-$ calcd for $C_{10}H_6FO$ 161.0408; found 161.0407. The spectroscopic data are consistent with those reported in the literature.[84]

*3-(Ethylamino)phenol (**7**).* The compound was prepared by modification of a known procedure.[85] Ethyl iodide (6.5 mL, 80.9 mmol) was added to a mixture of 3-aminophenol (2.0 equiv, 17.6 g, 162 mmol) and K_2CO_3 (11.2 g, 80.9 mmol) in DMF (45 mL) under a nitrogen atmosphere. The reaction mixture was heated to 100 °C for 2 h under stirring. The reaction mixture was poured into water (500 mL) and extracted with ethyl acetate (2 × 200 mL). The ethyl acetate layer was washed with water (500 mL) and brine (300 mL). The organic layer was dried with anhydrous Na_2SO_4 and evaporated to yield amber oil. The crude material was purified by column chromatography with the use of a gradient of dichloromethane/ethyl acetate (6:1 to 3:2, v/v) as a mobile phase. Yield 6.8 g (61%). Pale yellow oil. ^{1}H NMR (300 MHz, $CDCl_3$): δ (ppm) 7.01 (t, J = 8.0 Hz, 1H), 6.26−6.12 (m, 2H), 6.11 (t, J = 2.3 Hz, 1H), 4.14 (bs, 2H, N*H* + O*H*), 3.13 (q, J = 7.2 Hz, 2H), 1.24 (t, J = 7.1 Hz, 3H). The spectroscopic data are consistent with those reported in the literature.[86]

*3-(Ethyl(3-hydroxyphenyl)amino)propane-1-sulfonic Acid (**8**).* The compound was prepared according to a known procedure.[72] 3-Ethylaminophenol (**7**, 6.35 g, 46.3 mmol) and 1,3-propanesultone (1.1 equiv, 6.19 g, 50.7 mmol) were dissolved in *i*-propanol (50 mL) and refluxed under a nitrogen atmosphere for 3 h. During the reflux, a white precipitate was formed. The reaction mixture was cooled to room temperature, and the precipitate was filtered and washed with methanol (30 mL) to remove any unreacted 1,3-propanesultone. The material was vacuum-dried to give a white powder, 10.1 g (84%). ^{1}H NMR (300 MHz, DMSO-d_6): δ (ppm) 11.43 (bs, 1H), 10.16 (bs, 1H), 7.36 (t, J = 8.0 Hz, 1H), 7.20−6.61 (m, 3H), 3.80−3.21 (bm, 4H), 2.61 (t, J = 6.7 Hz, 2H), 1.77 (bs, 2H), 0.98 (t, J = 7.1 Hz, 3H). The spectroscopic data are consistent with those reported in the literature.[72]

*3-((3-Hydroxyphenyl)amino)propane-1-sulfonic Acid (**9**).* The compound was prepared according to a known procedure.[87] A solution of 1,3-propanesultone (1.5 equiv, 7.30 g, 59.8 mmol) in *n*-butanol (20 mL) was added to a solution of 3-aminophenol (4.32 g, 39.6 mmol) in *n*-butanol (70 mL). The mixture was refluxed for 4 h. During the reflux, a gray precipitate was formed. The suspension was cooled down to room temperature and filtered, and solids were washed with cold methanol (2 × 40 mL) and vacuum-dried. Yield 11.5 g (75%; purity 60% determined by integration of ^{1}H NMR signals). Gray powder. The crude material was a mixture of the title compound and a disubstituted derivative **10**. This material was used directly in the next step without further purification. ^{1}H NMR (300 MHz, D_2O): δ (ppm) 7.49 (t, J = 8.2 Hz, 1H), 7.13−6.96 (m, 3H), 3.63 (t, J = 7.5 Hz, 2H), 3.07 (t, J = 7.3 Hz, 2H), 2.23 (p, J = 7.5 Hz, 2H). The spectroscopic data are consistent with those reported in the literature.[87]

*3,3′-((3-Hydroxyphenyl)azanediyl)bis(propane-1-sulfonic acid) (**10**).* The compound was prepared by modification of a known procedure.[87] The solution of crude **10** (60.0%, 1.0 equiv, 5.00 g, 13.0 mmol) and 1,3-propanesultone (2.5 equiv, 3.88 g, 31.8 mmol) in DMF (40 mL) was heated to 145 °C for 1 h and then to 100 °C overnight under stirring. The reaction was monitored by TLC (methanol/ethyl acetate, 1:2, v/v). DMF was evaporated under reduced pressure, and a residue was purified by silica get column chromatography with the use of a gradient of acetone/H_2O (15:1 to 1:1, v/v) as a mobile phase to provide a dark brown solid of the title compound. Yield 2.88 g (63%). ^{1}H NMR (300 MHz, D_2O): δ (ppm) 7.57 (t, J = 8.2 Hz, 1H), 7.23−7.01 (m, 3H), 3.83 (t, J = 8.0 Hz, 4H), 2.96 (t, J = 7.3 Hz, 4H), 2.01 (p, J = 7.5 Hz, 4H). The spectroscopic data are consistent with those reported in the literature.[87]

General Procedure A: Preparation of Nitrosophenols 11a−c. Aminophenol (3-diethylaminophenol, **8** or **10**, 90 mmol) was dissolved in a mixture of water (20 mL) and concn HCl (50 mL). The solution was cooled to 0 °C, and a solution of sodium nitrite (1.0 equiv, 90 mmol) in water (15 mL) was added dropwise over a period of 30 min. The mixture of concn HCl and water (2:1, v/v) was added when stirring was not possible (~20 mL). Stirring was continued at 0 °C for 1 h. The suspension was filtered, and the residue was dried under vacuum to yield a brown to orange powder, which was sufficiently pure for the next step. In the case of water-soluble derivatives (**8** and **10**), no precipitate was formed after the addition of sodium nitrite; therefore, the solution was evaporated to dryness and the residue was directly used in the next step.

*5-(Diethylamino)-2-nitrosophenol Hydrochloride (**11a**).* The compound was prepared according to general procedure A from 3-diethylaminophenol (14.9 g, 90.0 mmol). The pure sample was prepared by recrystallization. The crude material was dissolved in a small amount of methanol, filtered, and the filtrate was precipitated by the addition of diethyl ether while cooling to −20 °C. The precipitate was filtered, washed with diethyl ether, and vacuum-dried. Yield 15.4 g (74%). Dark orange powder. ^{1}H NMR (300 MHz, CD_3OD): δ (ppm) 7.72 (d, J = 10.4 Hz, 1H), 7.21 (dd, J = 10.5, 2.3 Hz, 1H), 6.42 (d, J = 2.5 Hz, 1H), 3.93 (dq, J = 25.5, 7.2 Hz, 4H), 1.40 (t, J = 7.2 Hz, 6H). ^{13}C{^{1}H} NMR (75 MHz, CD_3OD): δ (ppm) 167.2, 164.1, 145.9, 124.8, 121.0, 98.9, 14.6, 13.1. The spectroscopic data are consistent with those reported in the literature.[88]

*3-(Ethyl(3-hydroxy-4-nitrosophenyl)amino)propane-1-sulfonic Acid Hydrochloride (**11b**).*[72] The compound was prepared according to general procedure A from **8** (2.0 g, 7.71 mmol). Brown hygroscopic powder. The yield was not determined, and a crude residue was directly used in the next step.

*3,3′-((3-Hydroxy-4-nitrosophenyl)azanediyl)bis(propane-1-sulfonic acid) Hydrochloride (**11c**).* The compound was prepared according to general procedure A from **10** (2.10 g, 5.94 mmol). Brown hygroscopic powder. The yield was not determined, and a crude residue was directly used in the next step.

General Procedure B: Synthesis of Nile Red Derivatives. Compounds **11a−c** (1 equiv, 4.34 mmol) and variously substituted 1-naphthol (1 equiv, 4.34 mmol) were charged to a flask. DMF (20 mL) was added and the reaction mixture was stirred and heated to 150 °C for 4 h under a nitrogen atmosphere. DMF was evaporated under a reduced pressure, and the residue was purified by silica gel column chromatography. The obtained compound was further purified by recrystallization from a suitable mixture of solvents.

https://dx.doi.org/10.1021/acs.joc.9b03217
J. Org. Chem. XXXX, XXX, XXX−XXX

*9-(Diethylamino)-5H-benzo[a]phenoxazin-5-one (Nile red) (**12a**).* The compound was prepared according to general procedure B from **11a** (3.48 g, 15.1 mmol) and 1-naphthol (2.17 g, 15.1 mmol). The crude material was purified by gradient dichloromethane/ethyl acetate (10:1 to 2:1, v/v) column chromatography and then recrystallized from dichloromethane/hexane on a rotary evaporator to provide dark green crystals. Yield 0.99 g (21%). ^{1}H NMR (300 MHz, $CDCl_3$): δ (ppm) 8.66 (dd, J = 7.8, 0.9 Hz, 1H), 8.31 (dd, J = 7.7, 1.1 Hz, 1H), 7.72 (td, J = 7.6, 1.5 Hz, 1H), 7.65 (td, J = 7.5, 1.4 Hz, 1H), 7.62 (d, J = 9.1 Hz, 1H), 6.68 (dd, J = 9.1, 2.7 Hz, 1H), 6.48 (d, J = 2.7 Hz, 1H), 6.39 (s, 1H), 3.48 (q, J = 7.1 Hz, 4H), 1.27 (t, J = 7.1 Hz, 6H). ^{13}C{^{1}H} NMR (75 MHz, $CDCl_3$): δ (ppm) 183.8, 152.2, 150.9, 146.9, 140.0, 132.2, 131.9, 131.4, 131.2, 130.0, 125.8, 125.1, 123.9, 109.8, 105.8, 96.4, 45.2, 12.8. UV−vis (CH_3OH, $c = 1 \times 10^{-5}$ M): $\lambda_{max}(\varepsilon)$ = 264 (42200), 305 (11200), 553 (42100) nm (dm^3 mol^{-1} cm^{-1}). Fluorescence (CH_3OH, $A(\lambda_{max}(exc)) < 0.1$): $\lambda_{max}(em)$ = 640 nm, Φ_F = 0.51. The spectroscopic data are consistent with those reported in the literature.[89]

*9-(Diethylamino)-2-hydroxy-5H-benzo[a]phenoxazin-5-one (**12b**).* The compound was prepared according to general procedure B from **11a** (1.00 g, 4.34 mmol) and 1,6-dihydroxynaphthalene (0.694 g, 4.34 mmol). The crude material was purified by gradient dichloromethane/ethyl acetate (10:1 to 2:1, v/v) column chromatography and then recrystallized from dichloromethane/methanol on a rotary evaporator to provide a dark green powder. Yield 0.230 g (16%). ^{1}H NMR (300 MHz, DMSO-d_6): δ (ppm) 10.36 (s, 1H), 7.96 (d, J = 8.6 Hz, 1H), 7.87 (d, J = 2.3 Hz, 1H), 7.55 (d, J = 9.0 Hz, 1H), 7.08 (dd, J = 8.6, 2.4 Hz, 1H), 6.77 (d, J = 9.2 Hz, 1H), 6.60 (s, 1H), 6.13 (s, 1H), 3.48 (q, J = 6.9 Hz, 4H), 1.16 (t, J = 7.0 Hz, 6H). ^{13}C{^{1}H} NMR (75 MHz, DMSO-d_6): δ (ppm) 181.5, 160.5, 151.5, 150.6, 146.3, 138.7, 133.7, 130.7, 127.4, 123.8, 123.8, 118.3, 109.8, 108.1, 104.0, 96.0, 44.3, 12.4. HRMS (APCI$^+$) m/z: [M + H]$^+$ calcd for $C_{20}H_{19}N_2O_3$ 335.1390; found 335.1388. UV−vis (CH_3OH, $c = 9 \times 10^{-6}$ M): $\lambda_{max}(\varepsilon)$ = 266 (34000), 547 (42 100) nm (dm^3 mol^{-1} cm^{-1}). Fluorescence (CH_3OH, $A(\lambda_{max}(exc)) < 0.1$): $\lambda_{max}(em)$ = 637 nm, Φ_F = 0.50. The spectroscopic data are consistent with those reported in the literature.[88]

*9-(Diethylamino)-3-fluoro-5H-benzo[a]phenoxazin-5-one (**12c**).* The compound was prepared according to general procedure B from **11a** (435 mg, 1.89 mmol) and 7-fluoronaphthalene-1-ol (**2**, 306 mg, 1.89 mmol). The crude material was purified by gradient dichloromethane/ethyl acetate (10:1 to 2:1, v/v) column chromatography and then recrystallized from dichloromethane/hexane on a rotary evaporator to provide dark green crystals. Yield 130 mg (21%). Mp 214−218 °C. ^{1}H NMR (300 MHz, $CDCl_3$): δ (ppm) 8.66 (dd, J = 8.8, 5.3 Hz, 1H), 7.94 (dd, J = 9.3, 2.7 Hz, 1H), 7.61 (d, J = 9.1 Hz, 1H), 7.46−7.33 (m, 1H), 6.69 (dd, J = 9.1, 2.7 Hz, 1H), 6.49 (d, J = 2.7 Hz, 1H), 6.41 (s, 1H), 3.48 (q, J = 7.1 Hz, 4H), 1.27 (t, J = 7.1 Hz, 6H). ^{19}F NMR (282 MHz, $CDCl_3$): δ (ppm) −109.03 (td, J = 8.7, 5.3 Hz). ^{13}C{^{1}H} NMR (75 MHz, $CDCl_3$): δ (ppm) 182.5 (d, J_{C-F} = 2.1 Hz), 164.2 (d, $^1J_{C-F}$ = 251.5 Hz), 152.3, 151.0, 146.9, 139.1 (d, J_{C-F} = 1.4 Hz), 134.1 (d, J_{C-F} = 7.5 Hz), 131.2, 128.5 (d, J_{C-F} = 2.8 Hz), 126.7 (d, J_{C-F} = 8.3 Hz), 125.2, 119.3 (d, J_{C-F} = 23.3 Hz), 111.7 (d, J_{C-F} = 22.9 Hz), 110.1, 105.8, 96.4, 45.3, 12.8. FTIR (neat, cm^{-1}): 3063, 2969, 2926, 1623, 1601, 1584, 1563, 1515, 1488, 1448, 1403, 1320, 1277, 1245, 1179, 1099, 1077, 1053, 1017, 922, 845, 830, 799, 619. HRMS (APCI$^+$) m/z: [M + H]$^+$ calcd for $C_{20}H_{18}FN_2O_2$ 337.1347; found 337.1348. UV−vis (CH_3OH, $c \sim 9.5 \times 10^{-5}$ M): $\lambda_{max}(\varepsilon)$ = 266 (10200), 304 (2470), 557 (11700) nm (dm^3 mol^{-1} cm^{-1}). Fluorescence (CH_3OH, $A(\lambda_{max}(exc)) < 0.1$): $\lambda_{max}(em)$ = 643 nm, Φ_F = 0.44.

*9-(Diethylamino)-3-hydroxy-5H-benzo[a]phenoxazin-5-one (**12d**).* The compound was prepared according to general procedure B from **11a** (1.17 g, 5.05 mmol) and 1,7-dihydroxynaphthalene (0.809 g, 5.05 mmol). The crude material was purified by gradient dichloromethane/ethyl acetate (10:1 to 2:1, v/v) column chromatography and then recrystallized from dichloromethane/methanol on a rotary evaporator to provide a fine green powder. Yield 0.370 g (26%). The number of peaks and coupling constants (^{1}H NMR) are consistent with those reported in the literature;[90] however, the chemical shifts of some aromatic peaks differ by up to 1 ppm compared to the reported data. ^{1}H NMR (300 MHz, DMSO-d_6): δ (ppm) 10.32 (s, 1H), 8.41 (d, J = 8.6 Hz, 1H), 7.58 (d, J = 9.0 Hz, 1H), 7.45 (d, J = 2.6 Hz, 1H), 7.21 (dd, J = 8.7, 2.7 Hz, 1H), 6.80 (dd, J = 9.2, 2.7 Hz, 1H), 6.63 (d, J = 2.7 Hz, 1H), 6.25 (s, 1H), 3.48 (q, J = 7.0 Hz, 4H), 1.16 (t, J = 6.9 Hz, 6H).^{13}C{^{1}H} NMR (75 MHz, DMSO-d_6): δ (ppm) 181.8, 159.6, 151.3, 150.0, 145.9, 138.7, 132.9, 130.3, 125.7, 124.0, 123.3, 120.0, 110.0, 109.8, 104.5, 96.0, 44.3, 12.4. HRMS (APCI$^+$) m/z: [M + H]$^+$ calcd for $C_{20}H_{19}N_2O_3$ 335.1390; found 335.1391.

*9-(Diethylamino)-4-fluoro-5H-benzo[a]phenoxazin-5-one (**12e**).* The compound was prepared according to general procedure B from **11a** (498 mg, 2.16 mmol) and 8-fluoronaphthalene-1-ol (**6**, 365 mg, 2.16 mmol). The crude material was purified by gradient dichloromethane/ethyl acetate (10:1 to 2:1, v/v) column chromatography and then recrystallized from dichloromethane/hexane on a rotary evaporator. Yield 157 mg (22%). Black powder. Mp 202−206 °C. ^{1}H NMR (300 MHz, $CDCl_3$): δ (ppm) 8.48 (d, J = 8.0 Hz, 1H), 7.62 (td, J = 8.1, 4.9 Hz, 1H), 7.55 (d, J = 9.1 Hz, 1H), 7.33−7.23 (m, 1H), 6.64 (dd, J = 9.1, 2.7 Hz, 1H), 6.43 (d, J = 2.7 Hz, 1H), 6.27 (s, 1H), 3.46 (q, J = 7.1 Hz, 4H), 1.26 (t, J = 7.1 Hz, 6H). ^{19}F NMR (282 MHz, $CDCl_3$): δ (ppm) −114.22 (dd, J = 11.6, 4.8 Hz). ^{13}C{^{1}H} NMR (75 MHz, $CDCl_3$): δ (ppm) 182.3 (d, J_{C-F} = 1.6 Hz), 161.4 (d, $^1J_{C-F}$ = 263.1 Hz), 151.4, 151.1, 146.9, 139.1 (d, J_{C-F} = 4.0 Hz), 134.7 (d, J_{C-F} = 1.5 Hz), 132.0 (d, J_{C-F} = 10.0 Hz), 131.3, 125.0, 120.2 (d, J_{C-F} = 4.8 Hz), 120.0 (d, J_{C-F} = 4.0 Hz), 118.0 (d, J_{C-F} = 22.2 Hz), 109.9, 107.0, 96.4, 45.2, 12.8. FTIR (neat, cm^{-1}): 3074, 3056, 2969, 2927, 2867, 1623, 1604, 1586, 1491, 1432, 1354, 1297, 1284, 1252, 1241, 1105, 926, 859, 793, 759. HRMS (APCI$^+$) m/z: [M + H]$^+$ calcd for $C_{20}H_{18}FN_2O_2$ 337.1347; found 337.1347. UV−vis (CH_3OH, $c \sim 2 \times 10^{-5}$ M): $\lambda_{max}(\varepsilon)$ = 263 (29400), 308 (8930), 560 (33 000) nm (dm^3 mol^{-1} cm^{-1}). Fluorescence (CH_3OH, $A(\lambda_{max}(exc)) < 0.1$): $\lambda_{max}(em)$ = 647 nm, Φ_F = 0.46.

*9-(Diethylamino)-3-methoxy-5H-benzo[a]phenoxazin-5-one (**15**).* The compound was synthesized according to a literature procedure.[91] **12d** (207 mg, 619 μmol) and KOH (3.0 equiv, 104 mg, 1.86 mmol) were charged in a flask. DMF (10 mL) was added under a nitrogen atmosphere followed by the addition of CH_3I (6.0 equiv, 230 μL, 3.71 mmol). The reaction mixture was stirred at room temperature for 40 min. The reaction progress was monitored by TLC (dichloromethane/ethyl acetate, 2:1, v/v). The solvent was evaporated, and the residue was purified by column chromatography eluting with dichloromethane/ethyl acetate (5:1, v/v). The crude product was recrystallized from dichloromethane/hexane on evaporator to yield fine orange-red crystals. Yield 149 mg (69%). Mp 194−197 °C. ^{1}H NMR (300 MHz, $CDCl_3$): δ (ppm) 8.56 (d, J = 8.8 Hz, 1H), 7.74 (d, J = 2.8 Hz, 1H), 7.59 (d, J = 9.0 Hz, 1H), 7.26 (dd, J = 8.8, 2.7 Hz, 1H), 6.67 (dd, J = 9.1, 2.7 Hz, 1H), 6.48 (d, J = 2.7 Hz, 1H), 6.39 (s, 1H), 3.96 (s, 3H), 3.46 (q, J = 7.1 Hz, 4H), 1.26 (t, J = 7.1 Hz, 6H). ^{13}C{^{1}H} NMR (75 MHz, $CDCl_3$): δ (ppm) 183.5, 161.6, 151.9, 150.4, 146.6, 140.0, 133.6, 130.9, 125.9, 125.5, 125.2, 120.4, 109.8, 107.2, 105.7, 96.5, 55.8, 45.2, 12.8. FTIR (neat, cm^{-1}): 3072, 3003, 2972, 2929, 2867, 2835, 1621, 1588, 1564, 1515, 1494, 1405, 1343, 1310, 1259, 1115, 1066, 1017, 851, 830, 794, 622. HRMS (APCI$^+$) m/z: [M + H]$^+$ calcd for $C_{21}H_{21}N_2O_3$ 349.1547; found 349.1547. UV−vis (CH_3OH, $c \sim 9.0 \times 10^{-6}$ M): $\lambda_{max}(\varepsilon)$ = 266 (39400), 300 (8180), 552 (43100) nm (dm^3 mol^{-1} cm^{-1}).

*3-(Ethyl(5-oxo-5H-benzo[a]phenoxazin-9-yl)amino)propane-1-sulfonic Acid (**13a**).* The compound was prepared according to general procedure B from **11b** (2.22 g, 7.70 mmol) and 1-naphthol (1.11 g, 7.70 mmol). The crude material was purified by column chromatography using ethyl acetate/*i*-propanol/H_2O (4:2:1, v/v) as a mobile phase and then recrystallized from methanol/ethyl acetate on a rotary evaporator. Yield 0.740 g (28%). Green powder. Mp 191−194 °C. ^{1}H NMR (300 MHz, DMSO-d_6): δ (ppm) 8.58 (d, J = 7.8 Hz, 1H), 8.13 (d, J = 7.4 Hz, 1H), 7.93−7.76 (m, 1H), 7.76−7.67 (m, 1H), 7.62 (d, J = 9.0 Hz, 1H), 6.91 (dd, J = 9.1, 2.6 Hz, 1H), 6.73 (d, J = 2.5 Hz, 1H), 6.30 (s, 1H), 3.65−3.45 (m, 4H), 2.55−2.51 (m, 2H, overlap with solvent peak), 1.89 (p, J = 6.9 Hz, 2H), 1.16 (t, J = 6.9 Hz, 3H). ^{13}C{^{1}H} NMR (126 MHz, DMSO-d_6): δ (ppm) 181.9,

https://dx.doi.org/10.1021/acs.joc.9b03217
J. Org. Chem. XXXX, XXX, XXX−XXX

151.8, 151.1, 146.3, 138.2, 131.6, 131.5, 131.0, 130.8, 129.8, 125.0, 124.2, 123.3, 110.5, 104.5, 96.1, 49.2, 48.4, 44.8, 23.4, 12.2. FTIR (neat, cm^{-1}): 3442 (broad), 3064, 2970, 2929, 2891, 1617, 1581, 1555, 1515, 1490, 1459, 1408, 1366, 1347, 1309, 1272, 1253, 1224, 1179, 1132, 1110, 1077, 1046, 1004, 777. HRMS (ESI^-) m/z: $[M - H]^-$ calcd for $C_{21}H_{19}N_2O_5S$ 411.1020; found 411.1021. UV−vis (CH_3OH, $c \sim 1.6 \times 10^{-5}$ M): $\lambda_{max}(\varepsilon)$ = 264 (29100), 552 (30400) nm ($dm^3\ mol^{-1}\ cm^{-1}$). UV−vis (PBS 10 mM, I = 0.1 M, $c \sim 1.6 \times 10^{-5}$ M): $\lambda_{max}(\varepsilon)$ = 268 (33100), 564 (32900) nm ($dm^3\ mol^{-1}\ cm^{-1}$). Fluorescence (CH_3OH, $A(\lambda_{max}(exc)) < 0.1$): $\lambda_{max}(em)$ = 640 nm, Φ_F = 0.44. Fluorescence (PBS 10 mM, I = 0.1 M, $A(\lambda_{max}(exc)) < 0.1$): $\lambda_{max}(em)$ = 659 nm, Φ_F = 0.063.

*3-(Ethyl(2-hydroxy-5-oxo-5H-benzo[a]phenoxazin-9-yl)amino)-propane-1-sulfonic Acid (**13b**).* The compound was prepared according to general procedure B from **11b** (2.22 g, 7.70 mmol) and 1,6-dihydroxynaphthalene (1.23 g, 7.70 mmol). The crude material was purified by column chromatography using ethyl acetate/*i*-propanol/H_2O (2:2:1, v/v) as a mobile phase and then recrystallized from methanol/ethyl acetate on a rotary evaporator. Yield 0.560 g (17%). Dark violet powder. ^1H NMR (500 MHz, DMSO-d_6): δ (ppm) 10.38 (s, 1H), 7.96 (d, J = 8.6 Hz, 1H), 7.89 (d, J = 2.5 Hz, 1H), 7.56 (d, J = 9.0 Hz, 1H), 7.08 (dd, J = 8.6, 2.5 Hz, 1H), 6.86 (dd, J = 9.1, 2.7 Hz, 1H), 6.68 (d, J = 2.7 Hz, 1H), 6.14 (s, 1H), 3.55 (t, J = 7.9 Hz, 2H), 3.51 (q, J = 7.0 Hz, 2H), 2.55−2.49 (m, 2H, overlap with solvent peak), 1.89 (p, J = 7.3 Hz, 2H), 1.15 (t, J = 7.0 Hz, 3H). $^{13}C\{^1H\}$ NMR (126 MHz, DMSO-d_6): δ (ppm) 181.5, 160.5, 151.6, 151.0, 146.3, 138.6, 133.7, 130.7, 127.4, 123.9, 123.8, 118.3, 110.1, 108.1, 104.0, 96.2, 49.2, 48.4, 44.8, 23.4, 12.2. FTIR (neat, cm^{-1}): 3406 (broad), 2973, 2931, 1641, 1588, 1561, 1518, 1481, 1441, 1410, 1319, 1272, 1181, 1119, 1089, 1043, 910, 824. HRMS (ESI^-) m/z: $[M - H]^-$ calcd for $C_{21}H_{19}N_2O_6S$ 427.0969; found 427.0971. UV−vis (CH_3OH, $c \sim 1.5 \times 10^{-5}$ M): $\lambda_{max}(\varepsilon)$ = 264 (29 000), 549 (29800) nm ($dm^3\ mol^{-1}\ cm^{-1}$). UV−vis (PBS 10 mM, I = 0.1 M, $c \sim 1.5 \times 10^{-5}$ M): $\lambda_{max}(\varepsilon)$ = 262 (27200), 560 (25800) nm ($dm^3\ mol^{-1}\ cm^{-1}$). Fluorescence (CH_3OH, $A(\lambda_{max}(exc)) < 0.1$): $\lambda_{max}(em)$ = 637 nm, Φ_F = 0.54. Fluorescence (PBS 10 mM, I = 0.1 M, $A(\lambda_{max}(exc)) < 0.1$): $\lambda_{max}(em)$ = 655 nm, Φ_F = 0.097. The spectroscopic data are in agreement with those reported in the literature.[92]

*3,3′-((5-Oxo-5H-benzo[a]phenoxazin-9-yl)azanediyl)bis-(propane-1-sulfonic Acid) (**14a**).* The compound was prepared according to general procedure B from **11c** (2.27 g, 7.87 mmol) and 1-naphthol (1.14 g, 7.87 mmol). The crude material was purified by column chromatography using a gradient of ethyl acetate/*i*-propanol/H_2O (4:2:1 to 1:1:1, v/v) as a mobile phase and then recrystallized from methanol/ethyl acetate on a rotary evaporator. Yield 0.175 g (5%). Dark violet powder. Mp > 220 °C. ^1H NMR (300 MHz, DMSO-d_6): δ (ppm) 8.58 (dd, J = 8.0, 1.3 Hz, 1H), 8.13 (dd, J = 7.8, 1.4 Hz, 1H), 7.81 (td, J = 7.6, 1.5 Hz, 1H), 7.71 (td, J = 7.5, 1.4 Hz, 1H), 7.62 (d, J = 9.1 Hz, 1H), 6.97 (dd, J = 9.2, 2.6 Hz, 1H), 6.79 (d, J = 2.5 Hz, 1H), 6.31 (s, 1H), 3.57 (t, J = 7.8 Hz, 4H), 2.57−2.49 (m, 4H, overlap with solvent peak), 1.89 (p, J = 7.3 Hz, 4H). $^{13}C\{^1H\}$ NMR (75 MHz, DMSO-d_6): δ (ppm) 181.9, 151.9, 146.4, 131.6, 131.5, 130.8, 129.8, 127.5, 125.0, 124.3, 123.4, 123.4, 110.7, 104.5, 96.3, 92.9, 49.6, 48.4, 23.2. FTIR (neat, cm^{-1}): 3432, 3067, 2941, 2883, 1617, 1585, 1557, 1492, 1461, 1412, 1366, 1313, 1183, 1137, 1116, 1048, 1005. HRMS (ESI^-) m/z: $[M - H]^-$ calcd for $C_{22}H_{21}N_2O_8S_2$ 505.0745; found 505.0745. UV−vis (CH_3OH, $c \sim 1.3 \times 10^{-5}$ M): $\lambda_{max}(\varepsilon)$ = 264 (24700), 552 (24500) nm ($dm^3\ mol^{-1}\ cm^{-1}$). UV−vis (PBS 10 mM, I = 0.1 M, $c \sim 1.3 \times 10^{-5}$ M): $\lambda_{max}(\varepsilon)$ = 267 (24800), 573 (25900) nm ($dm^3\ mol^{-1}\ cm^{-1}$). Fluorescence (CH_3OH, $A(\lambda_{max}(exc)) < 0.1$): $\lambda_{max}(em)$ = 640 nm, Φ_F = 0.55. Fluorescence (PBS 10 mM, I = 0.1 M, $A(\lambda_{max}(exc)) < 0.1$): $\lambda_{max}(em)$ = 654 nm, Φ_F = 0.19.

*3,3′-((2-Hydroxy-5-oxo-5H-benzo[a]phenoxazin-9-yl)azanediyl)-bis(propane-1-sulfonic Acid) (**14b**).* The compound was prepared according to general procedure B from **11c** (1.80 g, 4.71 mmol) and 1,6-dihydroxynaphthalene (0.754 g, 4.71 mmol). The crude material was purified by column chromatography using ethyl acetate/*i*-propanol/H_2O (1:1:2 v/v) as a mobile phase and then recrystallized from methanol/ethyl acetate on a rotary evaporator. Yield 0.200 g (8%). Dark violet powder. Mp > 220 °C. ^1H NMR (500 MHz, DMSO-d_6): δ (ppm) 10.39 (s, 1H), 7.96 (d, J = 8.6 Hz, 1H), 7.91 (d, J = 2.5 Hz, 1H), 7.55 (d, J = 9.1 Hz, 1H), 7.08 (dd, J = 8.6, 2.5 Hz, 1H), 6.92 (dd, J = 9.1, 2.7 Hz, 1H), 6.74 (d, J = 2.6 Hz, 1H), 6.15 (s, 1H), 3.56 (t, J = 7.8 Hz, 4H), 2.54−2.51 (m, 4H, overlap with solvent peak), 1.88 (p, J = 7.4 Hz, 4H). $^{13}C\{^1H\}$ NMR (126 MHz, DMSO-d_6): δ (ppm) 181.5, 160.5, 151.6, 151.2, 146.3, 138.6, 133.7, 130.6, 127.4, 123.9, 118.3, 110.3, 108.1, 104.0, 99.5, 96.3, 49.5, 48.4, 23.2. FTIR (neat, cm^{-1}): 3443, 3249, 2932, 2884, 1622, 1590, 1562, 1516, 1470, 1409, 1321, 1166, 1118, 1042, 911, 821, 741, 587, 521. HRMS (ESI^-) m/z: $[M - H]^-$ calcd for $C_{22}H_{21}N_2O_9S_2$ 521.0694; found 521.0696. UV−vis (CH_3OH, $c \sim 1.3 \times 10^{-5}$ M): $\lambda_{max}(\varepsilon)$ = 262 (21300), 546 (20200) nm ($dm^3\ mol^{-1}\ cm^{-1}$). UV−vis (PBS 10 mM, I = 0.1 M, $c \sim 1.3 \times 10^{-5}$ M): $\lambda_{max}(\varepsilon)$ = 261 (30600), 561 (27400) nm ($dm^3\ mol^{-1}\ cm^{-1}$). Fluorescence (CH_3OH, $A(\lambda_{max}(exc)) < 0.1$): $\lambda_{max}(em)$ = 637 nm, Φ_F = 0.60. Fluorescence (PBS 10 mM, I = 0.1 M, $A(\lambda_{max}(exc)) < 0.1$): $\lambda_{max}(em)$ = 652 nm, Φ_F = 0.13.

General Procedure C: Synthesis of Pd Sensors. This general procedure was optimized by modification of literature procedures.[40,55,56] Nile red derivative (**12**−**15**, 1.0 equiv, 400 μmol) and recrystallized $Pd(OAc)_2$ (1.0−2.0 equiv) were placed in a flask, and acetic acid (20 mL) was added under a nitrogen atmosphere. The mixture was stirred for 16 h at 65 °C. Acetic acid was evaporated under reduced pressure, and the residue was recrystallized from a suitable mixture of solvents on a rotary evaporator (the solution was filtered through a pad of Celite prior to recrystallization) to provide a Pd complex as a dark violet-blue powder.

*[(9-(Diethylamino)-5H-benzo[a]phenoxazin-5-one)Pd(μ-OAc)]$_2$ (**16a**).* The compound was prepared according to general procedure C from **12a** (141 mg, 443 μmol) and $Pd(OAc)_2$ (114 mg, 508 μmol). The residue was recrystallized from dichloromethane/hexane and then washed with diethyl ether (3 × 10 mL) on the frit to remove unreacted starting material. The title compound is insoluble in diethyl ether and hexane; on the other hand, starting material is soluble in both dichloromethane and diethyl ether. Yield 150 mg (70%). Dark blue powder. ^1H NMR (500 MHz, $CDCl_3$): δ (ppm) 7.71 (d, J = 9.2 Hz, 2H), 7.37 (d, J = 7.6 Hz, 2H), 6.77 (d, J = 7.7 Hz, 2H), 6.59 (t, J = 7.6 Hz, 2H), 6.33 (dd, J = 9.4, 2.6 Hz, 2H), 6.17 (d, J = 2.7 Hz, 2H), 6.04 (s, 2H), 3.46 (q, J = 6.9 Hz, 8H), 2.28 (s, 6H), 1.29 (t, J = 7.1 Hz, 12H). $^{13}C\{^1H\}$ NMR (126 MHz, $CDCl_3$): δ (ppm) 184.5, 181.8, 150.4, 150.4, 149.1, 148.4, 147.3, 142.3, 133.9, 130.7, 128.4, 127.9, 123.2, 121.3, 109.2, 107.4, 97.2, 45.3, 25.1, 12.9. FTIR (neat, cm^{-1}): 3061, 2970, 2928, 2868, 1634, 1616, 1570, 1545, 1519, 1489, 1405, 1380, 1351, 1302, 1283, 1250, 1187, 1120, 1094, 1077, 1019, 846, 795, 770. HRMS ($APCI^+$) m/z: $[M + H]^+$ calcd for $C_{44}H_{41}N_4O_8Pd_2$ 967.1012; found 967.1060. UV−vis (CH_3OH/dichloromethane (9:1), $c \sim 1 \times 10^{-5}$ M): $\lambda_{max}(\varepsilon)$ = 610 (37900) nm ($dm^3\ mol^{-1}\ cm^{-1}$). Fluorescence (CH_3OH/dichloromethane (9:1), $A(\lambda_{max}(exc)) < 0.1$): $\lambda_{max}(em)$ = 715 nm, Φ_F = 0.080. The spectroscopic data are consistent with those reported in the literature.[40,55,56]

*[(9-(Diethylamino)-2-hydroxy-5H-benzo[a]phenoxazin-5-one)-Pd(μ-OAc)]$_2$ (**16b**).* The compound was prepared according to general procedure C from **12b** (57.6 mg, 172 μmol) and $Pd(OAc)_2$ (65.0 mg, 290 μmol). The residue was recrystallized from dichloromethane/hexane and then washed with diethyl ether (3 × 10 mL) on the frit. Yield 80 mg (93%). Dark blue powder. Mp > 220 °C. ^1H NMR (500 MHz, $CDCl_3$): δ (ppm) 8.18 (s, 2H), 7.42 (d, J = 8.4 Hz, 2H), 7.34 (d, J = 9.4 Hz, 2H), 6.27 (dd, J = 9.5, 2.7 Hz, 2H), 6.11−5.98 (m, 4H), 5.90 (s, 2H), 3.42 (q, J = 7.2 Hz, 8H), 2.19 (s, 6H), 1.26 (t, J = 7.1 Hz, 12H). $^{13}C\{^1H\}$ NMR (126 MHz, $CDCl_3$): δ (ppm) 183.5, 183.2, 163.8, 150.4, 150.1, 149.6, 146.8, 143.8, 128.3, 126.7, 124.5, 124.2, 122.7, 117.6, 109.1, 107.7, 97.4, 45.3, 24.1, 12.9. FTIR (neat, cm^{-1}): 3282, 2973, 2929, 2873, 1617, 1583, 1565, 1520, 1494, 1399, 1342, 1311, 1269, 1184, 1114, 1098, 1075, 929, 826, 795. HRMS ($APCI^+$) m/z: $[M + H]^+$ calcd for $C_{22}H_{21}N_2O_5Pd$ 499.0489; found 499.0492, dimer not observed. UV−vis (CH_3OH/dichloromethane (9:1), $c \sim 1 \times 10^{-5}$ M): $\lambda_{max}(\varepsilon)$ = 610 (33500) nm ($dm^3\ mol^{-1}$

https://dx.doi.org/10.1021/acs.joc.9b03217
J. Org. Chem. XXXX, XXX, XXX−XXX

cm^{-1}). Fluorescence (CH_3OH/dichloromethane (9:1), $A(\lambda_{max}(exc)) < 0.1$): $\lambda_{max}(em)$ = 718 nm, Φ_F = 0.010.

*[(9-(Diethylamino)-3-fluoro-5H-benzo[a]phenoxazin-5-one)Pd-(μ-OAc)]$_2$ (**16c**).* The compound was prepared according to general procedure C from **12c** (134 mg, 398 μmol) and $Pd(OAc)_2$ (100 mg, 445 μmol). The residue was recrystallized from dichloromethane/hexane and then washed with diethyl ether (3 × 10 mL) on the frit. Yield 82 mg (41%). Dark violet-blue powder. ^{13}C was not possible to resolve because of a low solubility of the compound in CD_2Cl_2 and splitting of the signals by fluorine. Mp > 220 °C. ^1H NMR (500 MHz, CD_2Cl_2): δ (ppm) 7.68 (d, *J* = 9.3 Hz, 2H), 7.01 (dd, *J* = 9.1, 1.9 Hz, 2H), 6.47 (dd, *J* = 9.4, 2.8 Hz, 2H), 6.41 (dd, *J* = 8.5, 1.9 Hz, 2H), 6.23 (d, *J* = 2.8 Hz, 2H), 5.95 (s, 2H), 3.48 (q, *J* = 7.3 Hz, 8H), 2.27 (s, 6H), 1.29 (t, *J* = 7.2 Hz, 12H). ^{19}F NMR (471 MHz, CD_2Cl_2): δ (ppm) −104.51 (s). FTIR (neat, cm^{-1}): 3070, 2974, 2928, 2870, 1634, 1617, 1577, 1548, 1520, 1492, 1439, 1408, 1384, 1349, 1316, 1282, 1240, 1183, 1118, 1078, 1060, 840, 796. HRMS (APCI$^+$) *m*/*z*: $[M + H]^+$ calcd for $C_{44}H_{39}F_2N_4O_8Pd_2$ 1003.0824; found 1003.0837. UV−vis (CH_3OH/dichloromethane (9:1), $c \sim 1 \times 10^{-5}$ M): $\lambda_{max}(\varepsilon)$ = 630 (32900) nm (dm^3 mol^{-1} cm^{-1}). Fluorescence (CH_3OH/dichloromethane (9:1), $A(\lambda_{max}(exc)) < 0.1$): $\lambda_{max}(em)$ = 717 nm, Φ_F = 0.065.

*[(9-(Diethylamino)-3-methoxy-5H-benzo[a]phenoxazin-5-one)-Pd(μ-OAc)]$_2$ (**19**).* The compound was prepared according to general procedure C from **15** (55.0 mg, 158 μmol) and $Pd(OAc)_2$ (69.0 mg, 307 μmol). The residue was recrystallized from dichloromethane/hexane and then washed with diethyl ether (3 × 10 mL) on the frit. Yield 60 mg (74%). Dark blue powder. ^1H NMR (500 MHz, $CDCl_3$): δ (ppm) 7.72 (d, *J* = 9.3 Hz, 2H), 6.86 (d, *J* = 2.3 Hz, 2H), 6.40 (dd, *J* = 9.4, 2.8 Hz, 2H), 6.28 (d, *J* = 2.3 Hz, 2H), 6.22 (d, *J* = 2.7 Hz, 2H), 6.00 (s, 2H), 3.54 (s, 6H, OCH_3), 3.44 (q, *J* = 7.1 Hz, 8H), 2.27 (s, 6H), 1.27 (t, *J* = 7.2 Hz, 12H). $^{13}C\{^1H\}$ NMR (126 MHz, $CDCl_3$): δ (ppm) 184.3, 181.7, 159.4, 150.38, 150.37, 149.9, 148.3, 146.9, 135.8, 131.7, 127.7, 122.9, 120.7, 109.0, 107.1, 105.2, 97.0, 55.1, 45.0, 25.1, 12.8. HRMS (APCI$^+$) *m*/*z*: $[M + H]^+$ calcd for $C_{46}H_{45}N_4O_{10}Pd_2$ 1027.1224; found 1027.1216.

*[(3-(Ethyl(5-oxo-5H-benzo[a]phenoxazin-9-yl)amino)propane-1-sulfonic acid)Pd(μ-OAc)]$_2$ (**17a**).* The compound was prepared according to general procedure C from **13a** (150 mg, 364 μmol) and $Pd(OAc)_2$ (101 mg, 450 μmol). The residue was sonicated in dichloromethane (10 mL) and then filtered. The solid was dissolved in methanol (50 mL) and then filtered through a pad of Celite, and title compound was obtained by addition of dichloromethane (100 mL) to this solution and filtering of precipitated solids. We were not able to interpret the NMR spectra because of a strong broadening of peaks (in different solvents and at different temperatures). Yield 60 mg (29%). Dark blue powder. Mp > 220 °C. ^1H NMR (300 MHz, CD_3OD, a strong signal broadening): δ (ppm) 7.59, 7.25, 6.62, 6.28, 5.83, 5.48, 3.62, 3.55, 2.93, 2.16, 1.28, 1.28. FTIR (neat, cm^{-1}): 3412 (broad), 2970, 2929, 1627, 1571, 1538, 1488, 1404, 1277, 1128, 1037. HRMS (ESI$^-$) *m*/*z*: $[M - H]^-$ calcd for $C_{23}H_{21}N_2O_7PdS$ 575.0118; found 575.0082, a larger error is caused by averaging of the signals of monomer and dimer (see Figure S72).

*[(3-(Ethyl(2-hydroxy-5-oxo-5H-benzo[a]phenoxazin-9-yl)-amino)propane-1-sulfonic acid)Pd(μ-OAc)]$_2$ (**17b**).* The compound was prepared according to general procedure C from **13b** (100 mg, 364 μmol) and $Pd(OAc)_2$ (130 mg, 579 μmol). The residue was sonicated in dichloromethane (10 mL) and then filtered. The solid was dissolved in methanol (50 mL) and then filtered through a pad of Celite, and the title compound was obtained by the addition of dichloromethane (100 mL) to this solution and filtering of the precipitated solids. We were not able to interpret the NMR spectra because of a strong broadening of peaks (in different solvents and at different temperatures). Yield 66 mg (48%). Dark blue powder. Mp > 220 °C. NMR (300 MHz, DMSO-d_6): a strong signal broadening. HRMS (ESI$^-$) *m*/*z*: $[M - H]^-$ calcd for $C_{23}H_{21}N_2O_8PdS$ 591.0068; found 591.0064, dimer not observed.

*[(3,3′-((5-Oxo-5H-benzo[a]phenoxazin-9-yl)azanediyl)bis-(propane-1-sulfonic acid))Pd(μ-OAc)]$_2$ (**18a**).* The compound was prepared according to general procedure C from **14a** (50.0 mg, 98.7 μmol) and $Pd(OAc)_2$ (84.0 mg, 374 μmol). The residue was sonicated first in dichloromethane (10 mL), then in methanol (10 mL), and then filtered. The solid was dissolved in water (10 mL), then filtered through a pad of Celite, and the solvent was evaporated. We were not able to interpret the NMR spectra because of a strong broadening of peaks (in different solvents and at different temperatures). Yield 40 mg (60%). Dark blue powder. Mp > 220 °C. ^1H NMR (500 MHz, D_2O, a strong signal broadening): δ 7.09, 6.58, 6.49, 6.39, 6.22, 5.77, 3.61, 3.09, 3.07, 3.06, 2.23, 2.21, 2.19, 2.17, 2.16, 2.16. FTIR (neat, cm^{-1}): 3412 (broad), 2927, 1634, 1567, 1540, 1488, 1404, 1367, 1307, 1278, 1163, 1123, 1038, 797. HRMS (ESI$^-$) *m*/*z*: $[M - 2H]^{2-}$ calcd for $C_{24}H_{22}N_2O_{10}PdS_2$ 333.9885; found 333.9890, dimer not observed.

*[(3,3′-((2-Hydroxy-5-oxo-5H-benzo[a]phenoxazin-9-yl)-azanediyl)bis(propane-1-sulfonic acid))Pd(μ-OAc)]$_2$ (**18b**).* The compound was prepared according to general procedure C from **14b** (73.0 mg, 140 μmol) and $Pd(OAc)_2$ (138 mg, 615 μmol). The residue was sonicated first in dichloromethane (10 mL), then in methanol (10 mL), and then filtered. The solid was dissolved in water (10 mL), then filtered through a pad of Celite, and solvent was evaporated. We were not able to interpret the NMR spectra because of a strong broadening of peaks (in different solvents and at different temperatures). Mp > 220 °C. NMR (300 MHz, DMSO-d_6): a strong signal broadening. FTIR (neat, cm^{-1}): 3421, 2930, 1634, 1575, 1402, 1317, 1171, 1120, 1039. HRMS (ESI$^-$) *m*/*z*: $[M - H]^-$ calcd for $C_{24}H_{23}N_2O_{11}PdS_2$ 684.9784, found 684.9771, dimer not observed.

Synthesis of Trifluoroacetate Complex 20. *[(9-(Diethylamino)-5H-benzo[a]phenoxazin-5-one)Pd(μ-OOCCF$_3$)]$_2$ (**20**).* Nile red (**12a**, 50.0 mg, 157 μmol) and recrystallized $Pd(OAc)_2$ (1.2 equiv, 42.3 mg, 188 μmol) were charged in a flask, and trifluoroacetic acid (10 mL) was added. The mixture was stirred under a nitrogen atmosphere for 16 h at 65 °C. After cooling down to room temperature, a sufficient amount of diethyl ether (100 mL) was added, which caused precipitation. A dark blue-green solid was filtered, and the crude material (trifluoroacetate salt of the title compound) was redissolved in acetone. Anhydrous K_2CO_3 (∼0.5 g) was added to the solution, and the suspension was stirred for 1 h at room temperature. Acetone was evaporated, and the residue was redissolved in dichloromethane (50 mL) and filtered. The same volume of hexane was added to the mixture, and the major part of dichloromethane was evaporated under reduced pressure, which caused precipitation. The solid was filtered and washed with diethyl ether (2 × 10 mL) and hexane (2 × 10 mL). The residue was dried under vacuum. Yield 40 mg (47%). Dark blue solid. Mp > 220 °C. ^1H NMR (300 MHz, CD_2Cl_2): δ (ppm) 7.33 (d, *J* = 7.3 Hz, 2H), 7.29 (d, *J* = 9.3 Hz, 2H), 6.60−6.42 (m, 4H), 6.39 (dd, *J* = 9.4, 2.7 Hz, 2H), 6.17 (d, *J* = 2.7 Hz, 2H), 5.80 (s, 2H), 3.47 (q, *J* = 7.2 Hz, 8H), 1.27 (t, *J* = 7.1 Hz, 12H). ^{19}F NMR (471 MHz, $CDCl_3$): δ (ppm) -74.62 (s). $^{13}C\{^1H\}$ NMR (126 MHz, $CDCl_3$): δ (ppm) 183.7, 165.9 (q, $^2J_{C-F}$ = 38.7 Hz), 150.8, 149.8, 147.6, 147.1, 146.5, 141.8, 132.4, 130.7, 128.0, 127.5, 122.5, 121.9, 115.4 (q, $^1J_{C-F}$ = 287.4 Hz), 109.5, 107.4, 97.3, 45.4, 12.8. FTIR (neat, cm^{-1}): 3066, 2972, 2929, 2872, 1659, 1634, 1616, 1574, 1546, 1520, 1491, 1407, 1347, 1279, 1196, 1184, 1117, 1091, 1075, 1018, 846, 795, 767, 730. HRMS (APCI$^+$) *m*/*z*: $[M + H]^+$ calcd for $C_{44}H_{35}F_6N_4O_8Pd_2$ 1075.0447; found 1075.0462. UV−vis (CH_3OH/dichloromethane (9:1), $c \sim 1 \times 10^{-5}$ M): $\lambda_{max}(\varepsilon)$ = 616 (24500) nm (dm^3 mol^{-1} cm^{-1}). Fluorescence (CH_3OH/dichloromethane (9:1), $A(\lambda_{max}(exc)) < 0.1$): $\lambda_{max}(em)$ = 716 nm, Φ_F = 0.080.

General Procedure D: Preparative Synthesis of Methyl Ester Derivatives. A solution of palladacycle (**16a−c**, **19**, 7 μmol) in methanol (10 mL) was stirred under CO atmosphere for 16 h at room temperature. The black precipitate formed during the reaction (Pd black) was separated. The mixture was then filtered through a pad of Celite, and the filtrate was evaporated. The residue was purified by silica gel column chromatography to afford the methyl ester.

*Methyl 9-(Diethylamino)-5-oxo-5H-benzo[a]phenoxazine-1-carboxylate (**21a**).* The compound was prepared according to general procedure D from **16a** (200 mg, 207 μmol) and methanol (60 mL). Mobile-phase dichloromethane/ethyl acetate (2:1, v/v) was used for

https://dx.doi.org/10.1021/acs.joc.9b03217
J. Org. Chem. XXXX, XXX, XXX−XXX

purification. Yield 70 mg (45%). Black powder. Mp 184−188 °C. ^{1}H NMR (500 MHz, $CDCl_3$): δ (ppm) 8.41 (dd, J = 6.7, 2.6 Hz, 1H), 7.69−7.62 (m, 2H), 7.47 (d, J = 9.2 Hz, 1H), 6.65 (dd, J = 9.1, 2.7 Hz, 1H), 6.47 (d, J = 2.7 Hz, 1H), 6.40 (s, 1H), 4.00 (s, 3H), 3.46 (q, J = 7.1 Hz, 4H), 1.26 (t, J = 7.2 Hz, 6H). ^{13}C{^{1}H} NMR (126 MHz, $CDCl_3$): δ (ppm) 182.8, 171.4, 152.4, 151.4, 146.9, 138.1, 132.5, 131.6, 131.3, 130.4, 129.4, 128.7, 127.6, 124.5, 110.2, 105.7, 96.5, 52.4, 45.4, 12.7. FTIR (neat, cm^{-1}): 2963, 2945, 2924, 2869, 1733, 1615, 1581, 1562, 1489, 1468, 1414, 1358, 1311, 1268, 1242, 1179, 1113, 1070, 1017, 812, 774. HRMS (APCI$^+$) m/z: [M + H]$^+$ calcd for $C_{22}H_{21}N_2O_4$ 377.1496; found 377.1496. UV−vis (CH_3OH, $c \sim 1.3 \times 10^{-5}$ M): $\lambda_{max}(\varepsilon)$ = 268 (32100), 315 (7420), 561 (40100) nm (dm^3 mol^{-1} cm^{-1}). Fluorescence (CH_3OH, $A(\lambda_{max}(exc)) < 0.1$): $\lambda_{max}(em)$ = 635 nm, Φ_F = 0.54.

*Methyl 9-(Diethylamino)-2-hydroxy-5-oxo-5H-benzo[a]-phenoxazine-1-carboxylate (**21b**).* The compound was prepared according to general procedure D from **16b** (7.0 mg, 7.02 μmol). Dichloromethane/ethyl acetate (1:1, v/v) was used as a mobile phase. Yield was not determined (only an analytical amount was obtained). Dark violet solid. ^{1}H NMR (300 MHz, DMSO-d_6): δ (ppm) 10.82 (s, 1H), 8.07 (d, J = 8.6 Hz, 1H), 7.42 (d, J = 9.1 Hz, 1H), 7.23 (d, J = 8.7 Hz, 1H), 6.82 (dd, J = 9.2, 2.7 Hz, 1H), 6.64 (d, J = 2.6 Hz, 1H), 6.19 (s, 1H), 3.89 (s, 3H), 3.50 (q, J = 7.0 Hz, 4H), 1.16 (t, J = 6.8 Hz, 6H). HRMS (APCI$^+$) m/z: [M + H]$^+$ calcd for $C_{22}H_{21}N_2O_5$ 393.1445; found 393.1445.

*Methyl 9-(Diethylamino)-3-fluoro-5-oxo-5H-benzo[a]-phenoxazine-1-carboxylate (**21c**).* The compound was prepared according to general procedure D from **16c** (5.6 mg, 5.59 μmol). Dichloromethane/ethyl acetate (10:1, v/v) was used as a mobile phase. Yield was not determined (only an analytical amount was obtained). Dark black solid. ^{1}H NMR (300 MHz, $CDCl_3$): δ (ppm) 8.07 (dd, J = 8.8, 2.8 Hz, 1H), 7.47 (d, J = 9.1 Hz, 1H), 7.37 (dd, J = 7.8, 2.8 Hz, 1H), 6.68 (dd, J = 9.1, 2.7 Hz, 1H), 6.49 (d, J = 2.7 Hz, 1H), 6.42 (s, 1H), 4.01 (s, 3H), 3.48 (q, J = 7.1 Hz, 4H), 1.27 (t, J = 7.1 Hz, 6H). ^{19}F NMR (282 MHz, $CDCl_3$): δ (ppm) -108.51 (t, J = 8.3 Hz). HRMS (APCI$^+$) m/z: [M + H]$^+$ calcd for $C_{22}H_{20}FN_2O_4$ 395.1402; found 395.1402.

*Methyl 9-(Diethylamino)-3-methoxy-5-oxo-5H-benzo[a]-phenoxazine-1-carboxylate (**22**).* The compound was prepared according to general procedure D from **19** (7.0 mg, 6.83 μmol). The crude material was not purified by column chromatography. According to ^{1}H NMR and HRMS, the product of the reaction is a mixture of the title compound and **15** in the ratio of 1.4:1 (calculated from integration of ^{1}H NMR signals). Yield was not determined (only an analytical amount was obtained). Dark violet solid. ^{1}H NMR (title compound, 300 MHz, $CDCl_3$): δ (ppm) 7.86 (d, J = 2.7 Hz, 1H), 7.46 (d, J = 9.1 Hz, 1H), 7.21 (d, J = 2.7 Hz, 1H), 6.66 (dd, J = 9.1, 2.8 Hz, 1H), 6.48 (d, J = 2.7 Hz, 1H), 6.40 (s, 1H), 4.00 (s, 3H), 3.97 (s, 3H), 3.47 (q, J = 7.0 Hz, 4H), 1.26 (t, J = 7.1 Hz, 6H). HRMS (**22**, APCI$^+$) m/z: [M + H]$^+$ calcd for $C_{23}H_{23}N_2O_5$ 407.1601; found 407.1601. HRMS (**15**, APCI$^+$) m/z: [M + H]$^+$ calcd for $C_{21}H_{21}N_2O_3$ 349.1546; found 349.1547.

*Methyl-d_3 9-(Diethylamino)-5-oxo-5H-benzo[a]phenoxazine-1-carboxylate (**23**).* The compound was isolated from NMR kinetic measurements of the reaction of **16a** with CO in a CD_3OD/CD_2Cl_2 mixture. The solvent was evaporated, and the crude material was purified by silica gel column chromatography using dichloromethane/ethyl acetate (2:1, v/v) as a mobile phase. Yield was not determined (only an analytical amount of the product was obtained). Dark violet solid. ^{1}H NMR (300 MHz, $CDCl_3$): δ (ppm) 8.42 (dd, J = 6.0, 3.3 Hz, 1H), 7.73−7.58 (m, 2H), 7.47 (d, J = 9.1 Hz, 1H), 6.66 (dd, J = 9.1, 2.7 Hz, 1H), 6.47 (d, J = 2.7 Hz, 1H), 6.40 (s, 1H), 3.47 (q, J = 7.1 Hz, 4H), 1.26 (t, J = 7.0 Hz, 6H). ^{13}C{^{1}H} NMR (75 MHz, $CDCl_3$): δ (ppm) 182.8, 152.4, 151.4, 146.9, 138.2, 132.5, 131.6, 131.3, 130.4, 129.4, 128.7, 127.6, 124.5, 110.1, 105.7, 96.5, 45.3, 12.7. HRMS (APCI$^+$) m/z: [M + H]$^+$ calcd for $C_{22}H_{18}D_3N_2O_4$ 380.1684; found 380.1685.

■ ASSOCIATED CONTENT

Supporting Information

The Supporting Information is available free of charge at https://pubs.acs.org/doi/10.1021/acs.joc.9b03217.

NMR and optical spectra; HRMS, ESI-MS, SVD, and target analysis data; stability measurements; and fluorescence microscopy data (PDF)

■ AUTHOR INFORMATION

Corresponding Author

Petr Klán − *Department of Chemistry and RECETOX, Faculty of Science, Masaryk University, 625 00 Brno, Czech Republic;* orcid.org/0000-0001-6287-2742; Phone: +420-54949-4856; Email: klan@sci.muni.cz; Fax: +420-54949-2443

Authors

Dominik Madea − *Department of Chemistry and RECETOX, Faculty of Science, Masaryk University, 625 00 Brno, Czech Republic*

Marek Martínek − *Department of Chemistry and RECETOX, Faculty of Science, Masaryk University, 625 00 Brno, Czech Republic*

Lucie Muchová − *Institute of Medical Biochemistry and Laboratory Diagnostics, 1st Faculty of Medicine, Charles University, 121 08 Praha 2, Czech Republic*

Jiří Váňa − *Institute of Organic Chemistry and Technology, Faculty of Chemical Technology, University of Pardubice, 532 10 Pardubice, Czech Republic*

Libor Vítek − *Institute of Medical Biochemistry and Laboratory Diagnostics, 1st Faculty of Medicine, Charles University, 121 08 Praha 2, Czech Republic*

Complete contact information is available at: https://pubs.acs.org/10.1021/acs.joc.9b03217

Notes

The authors declare no competing financial interest.

■ ACKNOWLEDGMENTS

Support for this work was provided by the Czech Science Foundation (GA18-12477S). The authors thank Luboš Jílek and Peter Šebej (Masaryk University) for their help with the experiments and fruitful discussions and Miroslava Bittová (Masaryk University) for HRMS measurements.

■ REFERENCES

(1) Boczkowski, J.; Poderoso, J. J.; Motterlini, R. CO−metal interaction: vital signaling from a lethal gas. *Trends Biochem. Sci.* **2006**, *31*, 614−621.

(2) Townsend, C. L.; Maynard, R. L. Effects on health of prolonged exposure to low concentrations of carbon monoxide. *Occup. Environ. Med.* **2002**, *59*, 708−711.

(3) Ryter, S. W.; Alam, J.; Choi, A. M. K. Heme oxygenase-1/carbon monoxide: From basic science to therapeutic applications. *Physiol. Rev.* **2006**, *86*, 583−650.

(4) Wu, L.; Wang, R. Carbon Monoxide: Endogenous Production, Physiological Functions, and Pharmacological Applications. *Pharmacol. Rev.* **2005**, *57*, 585−630.

(5) Otterbein, L. E.; Bach, F. H.; Alam, J.; Soares, M.; Lu, H. T.; Wysk, M.; Davis, R. J.; Flavell, R. A.; Choi, A. M. K. Carbon monoxide has anti-inflammatory effects involving the mitogen-activated protein kinase pathway. *Nat. Med.* **2000**, *6*, 422−428.

(6) Motterlini, R.; Otterbein, L. E. The therapeutic potential of carbon monoxide. *Nat. Rev. Drug Discovery* **2010**, *9*, 728−743.

(7) Romão, C. C.; Blättler, W. A.; Seixas, J. D.; Bernardes, G. J. L. Developing drug molecules for therapy with carbon monoxide. *Chem. Soc. Rev.* **2012**, *41*, 3571−3583.
(8) Fernandez-Gonzalez, A.; Mitsialis, S. A.; Liu, X.; Kourembanas, S. Vasculoprotective effects of heme oxygenase-1 in a murine model of hyperoxia-induced bronchopulmonary dysplasia. *Am. J. Physiol.: Lung Cell. Mol. Physiol.* **2012**, *302*, L775−L784.
(9) Slanina, T.; Sebej, P. Visible-light-activated photoCORMs: rational design of CO-releasing organic molecules absorbing in the tissue-transparent window. *Photochem. Photobiol. Sci.* **2018**, *17*, 692−710.
(10) Heinemann, S. H.; Hoshi, T.; Westerhausen, M.; Schiller, A. Carbon monoxide - physiology, detection and controlled release. *Chem. Commun.* **2014**, *50*, 3644−3660.
(11) Schatzschneider, U. Photoactivated Biological Activity of Transition-Metal Complexes. *Eur. J. Inorg. Chem.* **2010**, 1451−1467.
(12) Schatzschneider, U. Novel lead structures and activation mechanisms for CO-releasing molecules (CORMs). *Br. J. Pharmacol.* **2015**, *172*, 1638−1650.
(13) Palao, E.; Slanina, T.; Muchova, L.; Solomek, T.; Vitek, L.; Klan, P. Transition-Metal-Free CO-Releasing BODIPY Derivatives Activatable by Visible to NIR Light as Promising Bioactive Molecules. *J. Am. Chem. Soc.* **2016**, *138*, 126−133.
(14) Romanski, S.; Kraus, B.; Schatzschneider, U.; Neudörfl, J.-M.; Amslinger, S.; Schmalz, H.-G. Acyloxybutadiene Iron Tricarbonyl Complexes as Enzyme-Triggered CO-Releasing Molecules (ET-CORMs). *Angew. Chem., Int. Ed.* **2011**, *50*, 2392−2396.
(15) Soboleva, T.; Berreau, L. M. 3-Hydroxyflavones and 3-Hydroxy-4-oxoquinolines as Carbon Monoxide-Releasing Molecules. *Molecules* **2019**, *24*, 1252.
(16) Šolomek, T.; Wirz, J.; Klan, P. Searching for Improved Photoreleasing Abilities of Organic Molecules. *Acc. Chem. Res.* **2015**, *48*, 3064−3072.
(17) Lee, Y.; Kim, J. Simultaneous electrochemical detection of nitric oxide and carbon monoxide generated from mouse kidney organ tissues. *Anal. Chem.* **2007**, *79*, 7669−7675.
(18) Park, S. S.; Kim, J.; Lee, Y. Improved Electrochemical Microsensor for the Real-Time Simultaneous Analysis of Endogenous Nitric Oxide and Carbon Monoxide Generation. *Anal. Chem.* **2012**, *84*, 1792−1796.
(19) Rimmer, R. D.; Richter, H.; Ford, P. C. A Photochemical Precursor for Carbon Monoxide Release in Aerated Aqueous Media. *Inorg. Chem.* **2010**, *49*, 1180−1185.
(20) Cao, Y.; Li, D. W.; Zhao, L. J.; Liu, X. Y.; Cao, X. M.; Long, Y. T. Highly Selective Detection of Carbon Monoxide in Living Cells by Palladacycle Carbonylation-Based Surface Enhanced Raman Spectroscopy Nanosensors. *Anal. Chem.* **2015**, *87*, 9696−9701.
(21) Motterlini, R.; Clark, J. E.; Foresti, R.; Sarathchandra, P.; Mann, B. E.; Green, C. J. Carbon monoxide-releasing molecules—Characterization of biochemical and vascular activities. *Circ. Res.* **2002**, *90*, E17−E24.
(22) Esteban, J.; Ros-Lis, J. V.; Martinez-Manez, R.; Marcos, M. D.; Moragues, M.; Soto, J.; Sancenon, F. Sensitive and Selective Chromogenic Sensing of Carbon Monoxide by Using Binuclear Rhodium Complexes. *Angew. Chem., Int. Ed.* **2010**, *49*, 4934−4937.
(23) Moragues, M. E.; Esteban, J.; Ros-Lis, J. V.; Martinez-Manez, R.; Marcos, M. D.; Martinez, M.; Soto, J.; Sancenon, F. Sensitive and Selective Chromogenic Sensing of Carbon Monoxide via Reversible Axial CO Coordination in Binuclear Rhodium Complexes. *J. Am. Chem. Soc.* **2011**, *133*, 15762−15772.
(24) Martínez-Máñez, R.; Sancenon, F. Fluorogenic and chromogenic chemosensors and reagents for anions. *Chem. Rev.* **2003**, *103*, 4419−4476.
(25) Wu, J. S.; Liu, W. M.; Ge, J. C.; Zhang, H. Y.; Wang, P. F. New sensing mechanisms for design of fluorescent chemosensors emerging in recent years. *Chem. Soc. Rev.* **2011**, *40*, 3483−3495.
(26) Pal, S.; Mukherjee, M.; Sen, B.; Mandal, S. K.; Lohar, S.; Chattopadhyay, P.; Dhara, K. A new fluorogenic probe for the selective detection of carbon monoxide in aqueous medium based on Pd(0) mediated reaction. *Chem. Commun.* **2015**, *51*, 4410−4413.
(27) Feng, W. Y.; Liu, D. D.; Feng, S. M.; Feng, G. Q. Readily Available Fluorescent Probe for Carbon Monoxide Imaging in Living Cells. *Anal. Chem.* **2016**, *88*, 10648−10653.
(28) Xu, Z. Y.; Yan, J. W.; Li, J.; Yao, P. F.; Tan, J. H.; Zhang, L. A colorimetric and fluorescent turn-on probe for carbon monoxide and imaging in living cells. *Tetrahedron Lett.* **2016**, *57*, 2927−2930.
(29) Feng, S. M.; Liu, D. D.; Feng, W. Y.; Feng, G. Q. Allyl Fluorescein Ethers as Promising Fluorescent Probes for Carbon Monoxide Imaging in Living Cells. *Anal. Chem.* **2017**, *89*, 3754−3760.
(30) Feng, W. Y.; Feng, G. Q. A readily available colorimetric and near-infrared fluorescent turn-on probe for detection of carbon monoxide in living cells and animals. *Sens. Actuators, B* **2018**, *255*, 2314−2320.
(31) Feng, W. Y.; Liu, D. D.; Zhai, Q. S.; Feng, G. Q. Lighting up carbon monoxide in living cells by a readily available and highly sensitive colorimetric and fluorescent probe. *Sens. Actuators, B* **2017**, *240*, 625−630.
(32) Yan, J. W.; Zhu, J. Y.; Tan, Q. F.; Zhou, L. F.; Yao, P. F.; Lu, Y. T.; Tan, J. H.; Zhang, L. Development of a colorimetric and NIR fluorescent dual probe for carbon monoxide. *RSC Adv.* **2016**, *6*, 65373−65376.
(33) Gong, S.; Hong, J.; Zhou, E.; Feng, G. A near-infrared fluorescent probe for imaging endogenous carbon monoxide in living systems with a large Stokes shift. *Talanta* **2019**, *201*, 40−45.
(34) Deng, Y.; Hong, J.; Zhou, E.; Feng, G. Near-infrared fluorescent probe with a super large Stokes shift for tracking CO in living systems based on a novel coumarin-dicyanoisophorone hybrid. *Dyes Pigm.* **2019**, *170*, No. 107634.
(35) Song, F. L.; Garner, A. L.; Koide, K. A highly sensitive fluorescent sensor for palladium based on the allylic oxidative insertion mechanism. *J. Am. Chem. Soc.* **2007**, *129*, 12354−12355.
(36) Yan, J. W.; Wang, X. L.; Zhou, L. F.; Zhang, L. CV-APC, a colorimetric and red-emitting fluorescent dual probe for the highly sensitive detection of palladium. *RCS Adv.* **2017**, *7*, 20369−20372.
(37) Michel, B. W.; Lippert, A. R.; Chang, C. J. A Reaction-Based Fluorescent Probe for Selective Imaging of Carbon Monoxide in Living Cells Using a Palladium-Mediated Carbonylation. *J. Am. Chem. Soc.* **2012**, *134*, 15668−15671.
(38) Zheng, K. B.; Lin, W. Y.; Tan, L.; Chen, H.; Cui, H. J. A unique carbazole-coumarin fused two-photon platform: development of a robust two-photon fluorescent probe for imaging carbon monoxide in living tissues. *Chem. Sci.* **2014**, *5*, 3439−3448.
(39) Li, Y.; Wang, X.; Yang, J.; Xie, X. L.; Li, M. M.; Niu, J. Y.; Tong, L. L.; Tang, B. Fluorescent Probe Based on Azobenzene-Cyclopalladium for the Selective Imaging of Endogenous Carbon Monoxide under Hypoxia Conditions. *Anal. Chem.* **2016**, *88*, 11154−11159.
(40) Liu, K. Y.; Kong, X. Q.; Ma, Y. Y.; Lin, W. Y. Rational Design of a Robust Fluorescent Probe for the Detection of Endogenous Carbon Monoxide in Living Zebrafish Embryos and Mouse Tissue. *Angew. Chem., Int. Ed.* **2017**, *56*, 13489−13492.
(41) Sun, M.; Yu, H.; Zhang, K.; Wang, S.; Hayat, T.; Alsaedi, A.; Huang, D. Palladacycle Based Fluorescence Turn-On Probe for Sensitive Detection of Carbon Monoxide. *ACS Sens.* **2018**, *3*, 285−289.
(42) Rogers, C. W.; Wolf, M. O. Drastic Luminescence Response to Carbon Monoxide from a RuII Complex Containing a Hemilabile Phosphane Pyrene Ether. *Angew. Chem., Int. Ed.* **2002**, *41*, 1898−1900.
(43) Wang, J.; Karpus, J.; Zhao, B. S.; Luo, Z.; Chen, P. R.; He, C. A Selective Fluorescent Probe for Carbon Monoxide Imaging in Living Cells. *Angew. Chem., Int. Ed.* **2012**, *51*, 9652−9656.
(44) Toscani, A.; Marín-Hernández, C.; Robson, J. A.; Chua, E.; Dingwall, P.; White, A. J. P.; Sancenón, F.; de la Torre, C.; Martínez-Máñez, R.; Wilton-Ely, J. D. E. T. Highly Sensitive and Selective Molecular Probes for Chromo-Fluorogenic Sensing of Carbon Monoxide in Air, Aqueous Solution and Cells. *Chem. - Eur. J.* **2019**, *25*, 2069−2081.

https://dx.doi.org/10.1021/acs.joc.9b03217
J. Org. Chem. XXXX, XXX, XXX−XXX

(45) Yan, T.; Chen, J.; Wu, S.; Mao, Z.; Liu, Z. A Rationally Designed Fluorescence Chemosensor for On-Site Monitoring of Carbon Monoxide in Air. *Org. Lett.* **2014**, *16*, 3296−3299.
(46) Shi, G.; Yoon, T.; Cha, S.; Kim, S.; Yousuf, M.; Ahmed, N.; Kim, D.; Kang, H.-W.; Kim, K. S. Turn-on and Turn-off Fluorescent Probes for Carbon Monoxide Detection and Blood Carboxyhemoglobin Determination. *ACS Sens.* **2018**, *3*, 1102−1108.
(47) Dhara, K.; Lohar, S.; Patra, A.; Roy, P.; Saha, S. K.; Sadhukhan, G. C.; Chattopadhyay, P. A New Lysosome-Targetable Turn-On Fluorogenic Probe for Carbon Monoxide Imaging in Living Cells. *Anal. Chem.* **2018**, *90*, 2933−2938.
(48) Tang, Z.; Song, B.; Ma, H.; Luo, T.; Guo, L.; Yuan, J. Mitochondria-Targetable Ratiometric Time-Gated Luminescence Probe for Carbon Monoxide Based on Lanthanide Complexes. *Anal. Chem.* **2019**, *91*, 2939−2946.
(49) Kaur, K.; Saini, R.; Kumar, A.; Luxami, V.; Kaur, N.; Singh, P.; Kumar, S. Chemodosimeters: An approach for detection and estimation of biologically and medically relevant metal ions, anions and thiols. *Coord. Chem. Rev.* **2012**, *256*, 1992−2028.
(50) Kumar, N.; Bhalla, V.; Kumar, M. Recent developments of fluorescent probes for the detection of gasotransmitters (NO, CO and H_2S). *Coord. Chem. Rev.* **2013**, *257*, 2335−2347.
(51) Zhang, C.; Xie, H.; Zhan, T.; Zhang, J.; Chen, B.; Qian, Z.; Zhang, G.; Zhang, W.; Zhou, J. A new mitochondrion targetable fluorescent probe for carbon monoxide-specific detection and live cell imaging. *Chem. Commun.* **2019**, *55*, 9444−9447.
(52) Repine, J. T.; Johnson, D. S.; White, A. D.; Favor, D. A.; Stier, M. A.; Yip, J.; Rankin, T.; Ding, Q.; Maiti, S. N. Synthesis of monofluorinated 1-(naphthalen-1-yl)piperazines. *Tetrahedron Lett.* **2007**, *48*, 5539−5541.
(53) Jurok, R.; Cibulka, R.; Dvořáková, H.; Hampl, F.; Hodačová, J. Planar Chiral Flavinium Salts—Prospective Catalysts for Enantioselective Sulfoxidation Reactions. *Eur. J. Org. Chem.* **2010**, *2010*, 5217−5224.
(54) Zhu, Z.; Colbry, N. L.; Lovdahl, M.; Mennen, K. E.; Acciacca, A.; Beylin, V. G.; Clark, J. D.; Belmont, D. T. Practical Alternative Synthesis of 1-(8-Fluoro-naphthalen-1-yl)piperazine. *Org. Process Res. Dev.* **2007**, *11*, 907−909.
(55) Aiello, I.; Ghedini, M.; La Deda, M. Synthesis and spectroscopic characterization of organometallic chromophores for photoluminescent materials: cyclopalladated complexes. *J. Lumin.* **2002**, *96*, 249−259.
(56) Liu, K. Y.; Kong, X. Q.; Ma, Y. Y.; Lin, W. Y. Preparation of a Nile Red-Pd-based fluorescent CO probe and its imaging applications in vitro and in vivo. *Nat. Protoc.* **2018**, *13*, 1020−1033.
(57) Hartwig, J. *Organotransition Metal Chemistry: From Bonding to Catalysis*; University Science Books: Sausalito, 2010.
(58) Tomazela, D.; Gozzo, F.; Ebeling, G.; Livotto, P.; N. Eberlin, M.; Dupont, J. On the Identification of Ionic Species of Neutral Halogen Dimmers and Pincer Type Palladacycles in Solution by Electrospray Mass and Tandem Mass Spectrometry. *Inorg. Chim. Acta* **2004**, *357*, 2349−2357.
(59) Otto, S.; Roodt, A.; Elding, L. I. Bridge-splitting kinetics, equilibria and structures of *trans*-biscyclooctene complexes of platinum(II). *Dalton Trans.* **2003**, 2519−2525.
(60) Ryabov, A. D. Cyclopalladated Complexes in Organic Synthesis. *Synthesis* **1985**, 233−252.
(61) Dupont, J.; Pfeffer, M.; Daran, J. C.; Jeannin, Y. Reactivity of cyclopalladated compounds. Part 17. Influence of the donor atom in metallacyclic rings on the insertion of *tert*-butyl isocyanide and carbon monoxide into their palladium-carbon bonds. X-ray molecular structure of cyclo-$[Pd(\eta(C,N)\text{-}\mu\text{-}C(C_6H_4CH_2SMe)=NBu\text{-}tert)Br]_2$. *Organometallics* **1987**, *6*, 899−901.
(62) Albert, J.; D'Andrea, L.; Granell, J.; Tavera, R.; Font-Bardia, M.; Solans, X. Synthesis and reactivity towards carbon monoxide of an optically active *endo* five-membered *ortho*-cyclopalladated imine: X-ray molecular structure of *trans*-$(\mu\text{-}Cl)_2[Pd(\kappa^2\text{-}C,N\text{-}(R)\text{-}C6H4\text{-}CH{=}N\text{-}CHMe\text{-}Ph]_2$. *J. Organomet. Chem.* **2007**, *692*, 3070−3080.
(63) Kretsinger, R. H.; Uversky, V. N.; Permyakov, E. A. Palladium Cytotoxicity. In *Encyclopedia of Metalloproteins*; Springer: NY, 2013; pp 1628.
(64) Wataha, J. C.; Hanks, C. T.; Craig, R. G. The in Vitro Effects of Metal Cations on Eukaryotic Cell Metabolism. *J. Biomed. Mater. Res.* **1991**, *25*, 1133−1149.
(65) Zuehlsdorff, T. J.; Haynes, P. D.; Payne, M. C.; Hine, N. D. M. Predicting solvatochromic shifts and colours of a solvated organic dye: The example of nile red. *J. Chem. Phys.* **2017**, *146*, No. 124504.
(66) Horváth, P.; Sebej, P.; Solomek, T.; Klan, P. Small-Molecule Fluorophores with Large Stokes Shifts: 9-Iminopyronin Analogues as Clickable Tags. *J. Org. Chem.* **2015**, *80*, 1299−1311.
(67) Cser, A.; Nagy, K.; Biczok, L. Fluorescence lifetime of Nile Red as a probe for the hydrogen bonding strength with its microenvironment. *Chem. Phys. Lett.* **2002**, *360*, 473−478.
(68) Ray, A.; Das, S.; Chattopadhyay, N. Aggregation of Nile Red in Water: Prevention through Encapsulation in β-Cyclodextrin. *ACS Omega* **2019**, *4*, 15−24.
(69) McGlynn, S. P.; Azumi, T.; Kinoshita, M. *Molecular Spectroscopy of the Triplet State*; Prentice-Hall: Englewood Cliffs, N.J., 1969.
(70) La Deda, M.; Ghedini, M.; Aiello, I.; Pugliese, T.; Barigelletti, F.; Accorsi, G. Organometallic emitting dyes: Palladium(II) nile red complexes. *J. Organomet. Chem.* **2005**, *690*, 857−861.
(71) Pugliese, T.; Godbert, N.; Aiello, I.; La Deda, M.; Ghedini, M.; Amati, M.; Belviso, S.; Lelj, F. Organometallic red-emitting chromophores: a computational and experimental study on cyclometallated Nile Red complexes of palladium(II) and platinum(II) acetylacetonates and hexafluoroacetylacetonates. *Dalton Trans.* **2008**, 6563−6572.
(72) Jose, J.; Burgess, K. Syntheses and Properties of Water-Soluble Nile Red Derivatives. *J. Org. Chem.* **2006**, *71*, 7835−7839.
(73) Nagy, K.; Göktürk, S.; Biczók, L. Effect of Microenvironment on the Fluorescence of 2-Hydroxy-Substituted Nile Red Dye: A New Fluorescent Probe for the Study of Micelles. *J. Phys. Chem. A* **2003**, *107*, 8784−8790.
(74) Maeder, M.; Neuhold, Y.-M. *Practical Data Analysis in Chemistry*; Elsevier: Amsterdam, 2007.
(75) Iacobucci, C.; Reale, S.; De Angelis, F. Elusive Reaction Intermediates in Solution Explored by ESI-MS: Reverse Periscope for Mechanistic Investigations. *Angew. Chem., Int. Ed.* **2016**, *55*, 2980−2993.
(76) Yunker, L. P. E.; Stoddard, R. L.; McIndoe, J. S. Practical approaches to the ESI-MS analysis of catalytic reactions. *J. Mass. Spectrom.* **2014**, *49*, 1−8.
(77) Liu; Takemura, F.; Yabe, A. Solubility and Diffusivity of Carbon Monoxide in Liquid Methanol. *J. Chem. Eng. Data* **1996**, *41*, 589−592.
(78) Cotton, J. D.; Crisp, G. T.; Daly, V. A. Alkyl substituent effects in ligand-induced carbon monoxide insertion reactions in $[(\eta^5\text{-}C_5H_5)(CO)_3Mo(benzyl)]$ systems. *Inorg. Chim. Acta* **1981**, *47*, 165−169.
(79) Martinek, M.; Filipova, L.; Galeta, J.; Ludviková, L.; Klan, P. Photochemical Formation of Dibenzosilacyclohept-4-yne for Cu-Free Click Chemistry with Azides and 1,2,4,5-Tetrazines. *Org. Lett.* **2016**, *18*, 4892−4895.
(80) Golub, G. H.; Pereyra, V. The Differentiation of Pseudo-Inverses and Nonlinear Least Squares Problems Whose Variables Separate. *SIAM J. Numer. Anal.* **1973**, *10*, 413−432.
(81) Newville, M.; Stensitzki, T.; Allen, D. B.; Ingargiola, A. *LMFIT: Non-Linear Least-Square Minimization and Curve-Fitting for Python*, version 0.8.0, Zenodo, 2014. http://doi.org/10.5281/zenodo.11813.
(82) Váňa, J.; Terencio, T.; Petrović, V.; Tischler, O.; Novák, Z.; Roithová, J. Palladium-Catalyzed C−H Activation: Mass Spectrometric Approach to Reaction Kinetics in Solution. *Organometallics* **2017**, *36*, 2072−2080.
(83) Sundalam, S. K.; Nilova, A.; Seidl, T. L.; Stuart, D. R. A Selective C−H Deprotonation Strategy to Access Functionalized

https://dx.doi.org/10.1021/acs.joc.9b03217
J. Org. Chem. XXXX, XXX, XXX−XXX

Arynes by Using Hypervalent Iodine. *Angew. Chem., Int. Ed.* **2016**, *55*, 8431−8434.
(84) Masson, E.; Schlosser, M. Fluoronaphthalene Building Blocks via Arynes: A Solution to the Problem of Positional Selectivity. *Eur. J. Org. Chem.* **2005**, *2005*, 4401−4405.
(85) Hirayama, R.; Kawase, M.; Kimachi, T.; Tanaka, K.; Yoneda, F. The autorecycling oxidation of benzylamine by synthetic 8-hydroxy-5-deazaflavin derivatives. *J. Heterocycl. Chem.* **1989**, *26*, 1255−1259.
(86) Yang, Z.; He, Y.; Lee, J.-H.; Park, N.; Suh, M.; Chae, W.-S.; Cao, J.; Peng, X.; Jung, H.; Kang, C.; Kim, J. S. A Self-Calibrating Bipartite Viscosity Sensor for Mitochondria. *J. Am. Chem. Soc.* **2013**, *135*, 9181−9185.
(87) Ho, N.-h.; Weissleder, R.; Tung, C.-H. Development of water-soluble far-red fluorogenic dyes for enzyme sensing. *Tetrahedron* **2006**, *62*, 578−585.
(88) Börgardts, M.; Verlinden, K.; Neidhardt, M.; Wöhrle, T.; Herbst, A.; Laschat, S.; Janiak, C.; Müller, T. J. J. Synthesis and optical properties of covalently bound Nile Red in mesoporous silica hybrids—comparison of dye distribution of materials prepared by facile grafting and by co-condensation routes. *RSC Adv.* **2016**, *6*, 6209−6222.
(89) Park, S.-Y.; Kubota, Y.; Funabiki, K.; Shiro, M.; Matsui, M. Near-infrared solid-state fluorescent naphthooxazine dyes attached with bulky dibutylamino and perfluoroalkenyloxy groups at 6- and 9-positions. *Tetrahedron Lett.* **2009**, *50*, 1131−1135.
(90) Ionescu, A.; Godbert, N.; Crispini, A.; Termine, R.; Golemme, A.; Ghedini, M. Photoconductive Nile red cyclopalladated metallomesogens. *J. Mater. Chem.* **2012**, *22*, 23617−23626.
(91) Brousmiche, D. W.; Serin, J. M.; Fréchet, J. M. J.; He, G. S.; Lin, T.-C.; Chung, S. J.; Prasad, P. N. Fluorescence Resonance Energy Transfer in a Novel Two-Photon Absorbing System. *J. Am. Chem. Soc.* **2003**, *125*, 1448−1449.
(92) Briggs, M. S.; Bruce, I.; Iller, J. N. M.; Moody, C. J.; Simmonds, A. C.; Swann, E. Synthesis of functionalised fluorescent dyes and their coupling to amines and amino acids. *J. Chem. Soc., Perkin Trans. 1* **1997**, 1051−1058.

https://dx.doi.org/10.1021/acs.joc.9b03217
J. Org. Chem. XXXX, XXX, XXX−XXX